NTNU

Norwegian University of
Science and Technology

Reservoir Characterization of Rogn Formation sandstones in the southern part of the Froan Basin Offshore Mid-Norway.

Subhan Gul Abbasi

Petroleum Geosciences
Submission date: July 2017
Supervisor: Mai Britt E. Mørk, IGP

Norwegian University of Science and Technology
Department of Geoscience and Petroleum

Abstract

Jurassic reservoirs offshore mid- Norway are of extreme importance in the Norwegian oil and gas sector. Petrophysical logs and thin sections of two cores from southern Froan Basin (Offshore mid-Norway) are investigated to understand the lithology, texture, sorting, grain size, reservoir properties and factors effecting these properties of the Rogn Formation sandstone. Petrophysical log data is used to interpret the lithology and calculate porosity/permeability of the interpreted lithology. Optical microscopy, XRD and modal analysis data is concatenated to explain rock types, grain size, texture, sorting, reservoir properties and diagenetic effects. The results from both methods are integrated and interpretations are made.

The sandstones unit is distinguished from the enclosing dark shales of the Spekk Formation in the petrophysical logs. The petrophysical logs are divided in to different zones based on different log responses. The sandstones are both texturally and compositionally sub mature to immature, and classifying as arkosic to subarkosic sandstones. The arkosic sandstone contains low mica and high microcline content whereas, sub-arkosic sandstone has a thickness of about 12 (m) and contains quartz, feldspar and high mica content. A general coarsening upward trend is established and the whole unit shows good reservoir properties with porosity ranging from 18 to 30% and permeability up to 340 milli-Darcy as calculated from petrophysical data.

The major factors effecting the reservoir properties are calcite cementation and authigenic clay cements. Early calcite cementation filled the primary pores and reduced the porosity of sandstone but also reduced the rate of mechanical compaction and obstructed quartz cementation to preserve porosity. Kaolinite is the abundant clay mineral and is formed because of feldspar alteration and dissolution. During uplifting episode, the meteoric water reacted with the Rogn Formation sandstone and late calcite cementation filled these secondary pores. Although the reservoir shows good properties, no hydrocarbon zone is identified from the logs in the study.

Acknowledgement

This project is a part of master's degree in Petroleum Geosciences at Department of Geology and Mineral Resources Engineering at NTNU. First, I would like to express my profound gratitude to my supervisor Professor Mai Britt E Mørk for valuable research guidance, comments during the work and for the time to proof read the report. My thanks also go to Professor Atle Mørk for his help and discussions.

I would like to express my special thanks of gratitude to Sintef petroleum Research As, for providing me with the Core data. I wish to present my appreciation to Laurentius Tijhuis for performing XRD.

At last but not the least I would like to thank my friends and family who helped me a lot during all these years.

Trondheim, 12th July 2017

Subhan Gul Abbasi

Table of Contents

CHAPTER 1 INTRODUCTION 1

1.1 Introduction 1
1.2 Objectives of the Project 1
1.3 Study Area 1
1.4 Previous studies 2

CHAPTER 2 DIAGENESIS AND DIAGENETIC REGIMES 5

2.1 Diagenesis 5
2.2 Stages of Diagenesis 5
2.2.1 Eogenesis 6
2.2.2 Mesogenesis (Burial diagenesis) 6
2.2.3 Telogenesis 7
2.3 Diagenetic Cements in sandstones 8

CHAPTER 3 GEOLOGY OF THE NORWEGIAN SEA 11

3.1 Tectonic Framework and history of the Norwegian Continental Margin 11
3.2 Structural Development 12
3.2.1 The Northern structural province 12
3.2.2 The middle Structural province 13
3.2.3 Southern Structural Province 13
3.3 Mesozoic Sediments and Structures in the Norwegian Sea 14
3.4 The Trøndelag Platform 15
3.4.1 Geology of the Trøndelag Platform 16
3.4.2 Froan Basin 17
3.4.3 Provenance of the Jurassic reservoirs in the Froan Basin 17
3.5 Lithopstratigraphy 18
3.5.1 Viking Group (Vikinggruppen) 19

CHAPTER 4 MATERIALS AND METHODOLOGY 23

4.1 Petrographical Analysis 23
4.1.1 Optical Microscopy 24
4.1.2 Core Photographs 24
4.1.3 X-ray Diffraction (XRD) 24
4.2 Petrophysical Analysis 25
4.2.1 Lithology Identification 25
4.2.2 Porosity and Permeability estimation 25

CHAPTER 5 RESULTS 27

5.1 Results Petrophysical Analysis 27
5.1.1 Well 6307/07-U-02 27
5.1.2 Neutron Density Cross plot and Grain-density histogram 32
5.1.3 Crossplot of Porosity-permeability 33
5.1.4 Well 6307/07-U-03A 34
5.2 Results Petrographical Analysis 37
5.2.1 Microscopy Results 37

5.2.2 Modal Analysis results *44*
5.2.3 X-ray Diffraction Results *47*

CHAPTER 6 DISCUSSIONS **51**

6.1 DIAGENETIC PROCESSES 51
6.2 DETRITAL GRAINS 52
6.3 TEXTURAL MATURITY 53
6.4 CLASSIFICATION OF SANDSTONES 54
6.5 POROSITY AND PERMEABILITY 54
6.6 POROSITY PRESERVING MECHANISM IN THE ROGN FORMATION 55
6.7 PROVENANCE AND DEPOSITIONAL ENVIRONMENT 56
6.8 RELATIONSHIP BETWEEN PETROPHYSICAL AND PETROGRAPHICAL ANALYSIS 57

CHAPTER 7 CONCLUSIONS **59**

REFERENCES **61**

APPENDIX A **65**

APPENDIX B **69**

List of Figures

Figure 1 Location of the Cores (red circle), main geological provinces and structural elements off Møre-Trøndelag. FB: Frohavet Basin, WGR: Western Gneiss Region, VFC: Vingleia Fault Complex, VF: Vingleia Fault, SS-b: Slørebotn Sub-basin, TNC: Trondheim Nappe Complex, MTFC: Møre-Trøndelag Fault Complex, KFC: Klakk Fault Complex, HSF: Hitra-Snåsa Fault (Mørk and Johnsen, 2005). 2

Figure 2 Shows the relationship between Diagenetic processes and metamorphism. The temperature gradients of 10°C km−1 and 30°C km−1 represents stable cratons and rifted basins respectively (Worden and Burley, 2003). 5

Figure 3 shows decrease of porosity with burial depth due to chemical and mechanical compaction(Boggs, 2006). 7

Figure 4 Flow chart diagram representing different diagenetic processes. The mesogenesis can grade on to telogenesis during any phase of burial because of uplift and erosion (Worden and Burley, 2003). 8

Figure 5 Regional tectonic setting of the Norwegian continental margin. YP: Yermak Plateau, GR: Greenland Ridge, JMR: Jan Mayen Ridge, MM: Møre Margin, VM: Vøring Margin, BF: Bjørnøya Fan, NSF: North Sea Fan, HR: Hovgård Ridge, VP: Vøring Plateau, LVM: Lofotebn-Vesterålen Margin, EGM: East Greenland Margin, SF: Storfjorden Fan (Faleide et al., 2008). 12

Figure 6 Major tectonic and structural elements of the Norwegian Sea continental margin (Brekke et al., 1999) 14

Figure 7 Geological map of Mid-Norway representing the Trøndelag Platform (Lundin et al., 2005) 16

Figure 8 Interpreted seismic profile of Froan Basin and Frøya High (Lundin et al., 2005). 18

Figure 9 Stratigraphy of the Vøring Basin, Halten Terrace and Trøndelag Platform (Brekke et al., 2001). 19

Figure 10 Shows the gamma ray response of the Spekk, Rogn and Melke formations. a) Well no:6407/9-1, b) 6506/12-4 (Halland et al., 2014) 22

Figure 11 Flow chart diagram of the project 23

Figure 12 Interpreted Petrophysical log of well 6307/07-U-02. The red dots are the core porosity and permeability value. GR (green), Caliper log (grey), Neutron Porosity log (blue), Density log (red), Sonic log (pink), Density porosity (black), Permeability, blue and red dots represent the core data. 31

Figure 13 Neutron-density crossplot and of well 6307/07-U-02. Where Neutron porosity is on x-axis and Density porosity on y-axis. 32

Figure 14 Grain-density histogram of well 6307/07-U-02 33

Figure 15 Porosity/permeability cross-plot 34

Figure 16 Interpreted petrophysical log of well 6307/07-U-03A. The red dots are representing the core data. Red dots represent the core data 36

Figure 17 Cross polar, optical micrograph image from 15.34 m. Major porosity resducing elements in the Rogn Formation sandstone. Cc: Calcite cement, Cly: Clay minerals. 38

Figure 18 Cross polar, optical micrograph image from 129.50 m. Arkosic sandstone showing dissoloution of feldspar and precipitation of kaolinite/calcite cement in the secondary pores. Plg: Plageoclase, Cly: Clay minerals, Qtz: quartz. 38

Figure 19 Cross polar (10x), Optical micrograph image from 181.55m. Arkosic sandstone showing compaction (mica bending) and high inter grannular volume. 39

FIGURE 20 POROSITY AND MINERALOGICAL COMPOSITION FROM MODAL ANALYSIS. HEAVY MINERALS ARE COUNTED IN ROCK FRAGMENTS. 46
FIGURE 21 DETRITAL GRAINS COMPOSITION FROM MODAL ANALYSIS AT DIFFERENT DEPTHS 46
FIGURE 22 COMPOSITION OF CARBONATE CEMENTS AND CLAY MINERALS FROM MODAL ANALYSIS AT DIFFERENT DEPTHS 47
FIGURE 23 TOTAL MINERALOGICAL COMPOSITION FROM XRD ANALYSIS. 49
FIGURE 24 PLAIN POLAR, OPTICAL MICROGRAPH IMAGE FROM 149.81 . ARKOSIC SANDSTONE (FELDSPAR RICH) OF ROGN FORMATION SANDSTONE. QUARTZ FELDSPAR ARE THE DETRITAL GRAINS DISSOLOUTION OF FELDSPAR CAN BE OBSERVED. 52
FIGURE 25 CLASSIFICATION OF TEXTURAL MATURITY (FOLK, 1951). 53
FIGURE 26 QTZ- FSPR-LITHCS PLOT OF THE ROGN FORMATION SANDSTONE SAMPLES (DOTT JR, 1964). 54
FIGURE 27 CROSS POLAR, OPTICAL MICROGRAPH IMAGE FROM 105.81 M. SUB-ARKOSIC SANDSTONE OF THE ROGN FORMATION. CC : CARBONATE CEMENT (CALCITE), QTZ: QUARTZ, FSPR: FELDSPAR, MICA (MUSCOVITE). MICA SHOWS MINOR BENDING DUE TO COMPACTION. 55
FIGURE 28 OPTICAL MICRO GRAPH IMAGE OF ORGANIC RICH SHALE (SPEKK FORMATION) FROM 80.97 M. 56

List of Tables

TABLE 1 LITHOLOGY AND AGES OF FORMATIONS IN THE VIKING GROUP. DATA USED IN THIS TABLE IS EXTRACTED FROM (DALLAND ET AL., 1988; VOLLSET AND DORÉ, 1984). A) NORTH SEA, B) NORWEGIAN SEA 20
TABLE 2 THE RESULTS OF THE PETROPHYSICAL ANALYSIS AND AVAILABILITY OF THIN SECTIONS AND XRD DATA 28
TABLE 3 ZONES AND LITHOLOGY OF WELL 6307/07-U-03A AND AVAILABILITY OF XRD AND THIN SECTION DATA. 35
TABLE 4 DESCRIPTION OF THIN SECTION SLIDES USED IN THE STUDY. A) SAMPLES OF LANGE AND SPEKK FORMATION FROM ZONE 1-5, B) SUB ARKOSIC SANDSTONE SAMPLES FROM ZONE 6 AND 7, C) ARKOSIC SANDSTONE SAMPLES FROM ZONE 8, D) ARKOSIC SANDSTONE SAMPLES FROM ZONE 9, E) SAMPLES FROM ZONE 10, F) SAMPLES FROM CORE 6307/07-U-02 39
TABLE 5 PETROGRAPHIC COMPOSITION OF SANDSTONE BASED ON MODAL ANALYSIS (300 POINTS, THE VALUES ARE IN PERCENTAGE). 45
TABLE 6 MINERALOGICAL COMPOSITION FROM XRD ANALYSIS. 49

Abbreviations

Alb	Albite
Cc	Calcite cement
Chl	chlorite
Chlpy	Chalcopyrite
Cly	Clay minerals
D	1Depth
Fspr	Feldspar
Glauc	Glauconite
HI	Hydrogen Index
Jrc	Jarocite
Kao	Kaolinite
Lith	Lithology
m	meter
IGV	Intergranular volume
mm	millimeter
Mus	Muscovite
NPHI	Neutron Porosity log
P	Porosity
Plg	Plageoclase
Py	Pyrite
Qrtz	Quartz
Rf	Rock fragment
Sid	Siderite
SN	Sample Number
Sst	Sandstone
XRD	X-ray diffraction

Chapter 1 Introduction

1.1 Introduction

Jurassic sandstones in the North Sea and Haltenbanken are the most important petroleum reservoirs offshore Norway. In offshore mid Norway, initially the Halten Terrace and nearby areas were the target of the exploration companies, i.e. most of the discoveries are in this area. 6507/12-1, which was the first well drilled offshore mid-Norway by Saga petroleum in 1980 helped understanding the potential plays (Dalland et al., 1988). On the Mid-Norway shelf the proven oil and gas reserves are l21.2 mill.Sm^3 and 380.2 billion.Sm^3 respectively. The successful story of the mid Norway shelf comes to a halt by seeing the facts that all the discoveries offshore mid Norway except Draugen are in the Haltenbanken area. 13 dry wells have been drilled away from the Halten Terrace structural element within 65°30' to 67°N, 13' until 1990 (Fagerland, 1990). The Exploration activities saw a dramatic rise and 74 discoveries have been made since 2000 (NPD, 2016).

In the Haltenbanken and Draugen fields middle to late Jurassic are the proven reservoirs. The organic rich source rock of the Upper Jurassic Spekk Formation is widely distributed over the Haltenbanken and Trøndelag area. A Jurassic sandstone (Rogn Formation) confined in the Spekk Formation is the producing reservoir in the Draugen field.

1.2 Objectives of the Project

The objective of this project is to investigate the reservoir quality of the Upper Jurassic Rogn Formation sandstone encountered in the Froan Basin area. The study involves description of the lithology, mineralogy, texture, grain size, sorting, porosity and permeability by combining petrophysical and petrographical techniques. The diagenetic processes and their impacts on the reservoir quality are also considered.

1.3 Study Area

A shallow coring program was initiated in 1988 by the Continental Shelf Institute (IKU), presently known as Sintef Petroleum Research AS. In this coring program, a total of 8 shallow stratigraphic cores were recovered at different locations offshore Møre-Trøndelag. While drilling on seismic line IKU-201-88 a total of 541 meters of cores is recovered (Smelror et al., 1994). Petrophysical logs and thin sections used in this study are from the two cores (6307/07-U-02 & U-03A) drilled in this program.

The cores (6307/07-U-02 & U-03) were drilled off mid Norway in the southern margin of the

Froan basin of the Møre-Trøndelag area (Fig. 1) and 80 meters of Rogn Formation (Upper Jurassic sandstones) within the Spekk Formation (shale) have been cored.

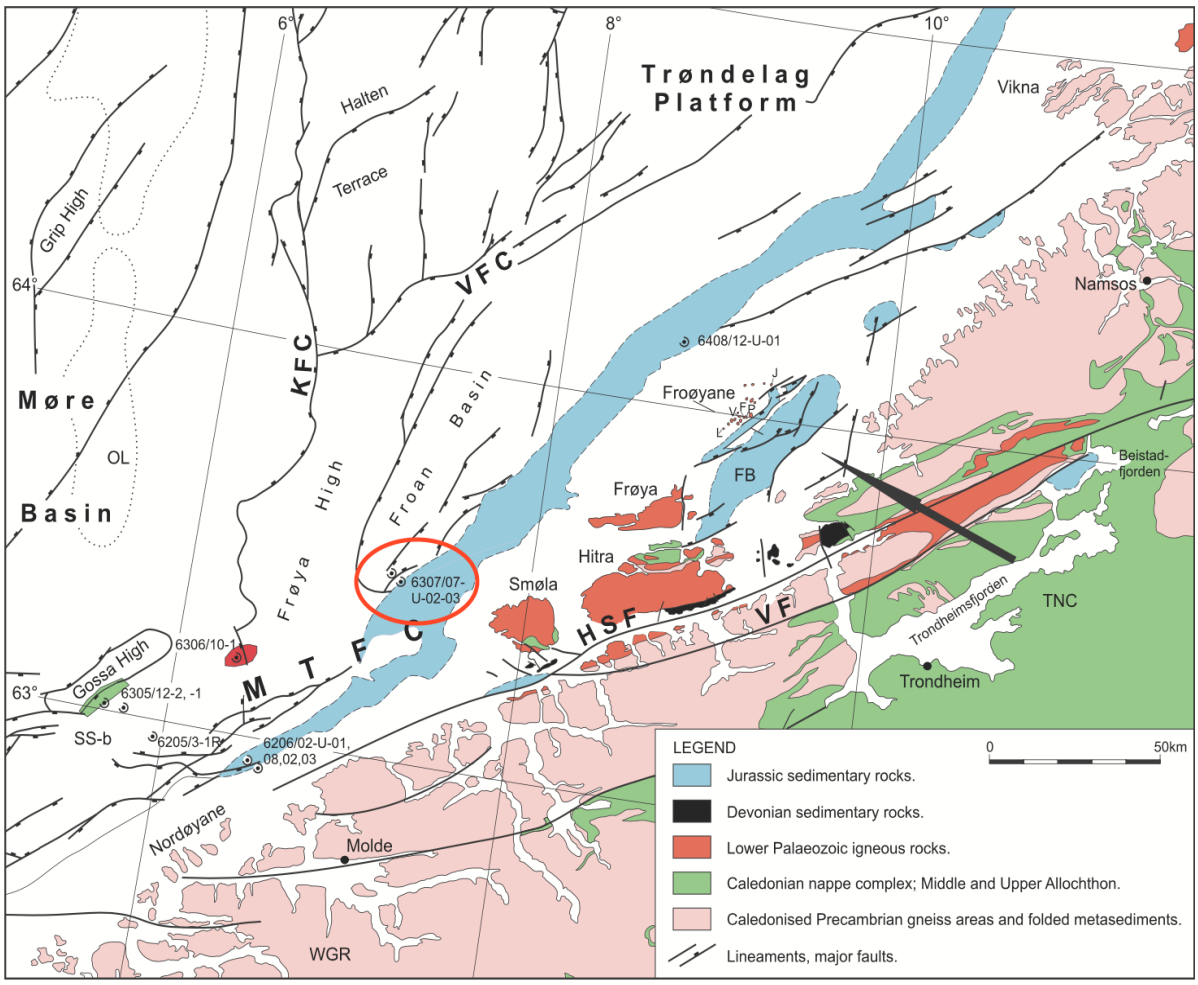

Figure 1 Location of the Cores (red circle), main geological provinces and structural elements off Møre-Trøndelag. FB: Frohavet Basin, WGR: Western Gneiss Region, VFC: Vingleia Fault Complex, VF: Vingleia Fault, SS-b: Slørebotn Sub-basin, TNC: Trondheim Nappe Complex, MTFC: Møre-Trøndelag Fault Complex, KFC: Klakk Fault Complex, HSF: Hitra-Snåsa Fault (Mørk and Johnsen, 2005).

1.4 Previous studies

Many geologists have extensively investigated the evolution and structural elements of the Norwegian continental margin. The major contributions in understanding the structures and tectonic elements of the Norwegian continental margin are by Aanstad et al. (1981), Bukovics et al. (1984), Brekke and Riis (1987), Blystad et al. (1995), Grogan et al. (1999), and Faleide et al. (2008). The sedimentology and stratigraphy of the Norwegian Sea is explained by Rhys, (1974), Deegan and Scull, (1977), Dalland et al. (1988), Isaksen and Tonstad, (1989), and Gjelberg, (2001). The Lithostratigraphic nomenclature for Mesozoic and Cenozoic sediments

in offshore mid and northern Norway is discussed by Dalland et al. (1988). Research on play based evaluation of the Trøndelag platform is carried out by Saxena, (2016).

The Trøndelag Platform is suitable for long-term storage of CO_2 because it is located near the coast and only short pipelines are needed for transportation. Lundin et al. (2005) reported the storage potential for CO_2 in the Froan Basin.

An interpretation of provenance of Jurassic sandstones in the study area is done by Mørk and Johnsen, (2005). This study reports a local provenance from different igneous and metamorphic rocks in Triassic to lower Jurassic deposits. It also suggests that Middle Jurassic and Upper Jurassic-Lower Cretaceous sediments have a provenance from erosion of Palaeozoic plutonic rocks.

Chapter 2 Diagenesis and Diagenetic Regimes

2.1 Diagenesis

Diagenesis refers to all the chemical, physical and biogenic processes that effect the original assemblage of the sedimentary rocks. The diagenetic process starts during and /or just after the deposition of sediments due to continuous changes in temperature, pressure and chemistry. The post depositional changes in the sediments are result of processes such as weathering, oxidation, compaction and lithification. Diagenetic changes occur at lower temperature and pressure than metamorphism from surface temperatures up to temperatures of 250°C as shown in Figure (2) (Boggs, 2006). Burial and uplifting of the basin subjects the sediments to different chemical and physical conditions from the initial depositional conditions and changes of temperature, pressure and pore fluid chemistry (Worden and Burley, 2003).

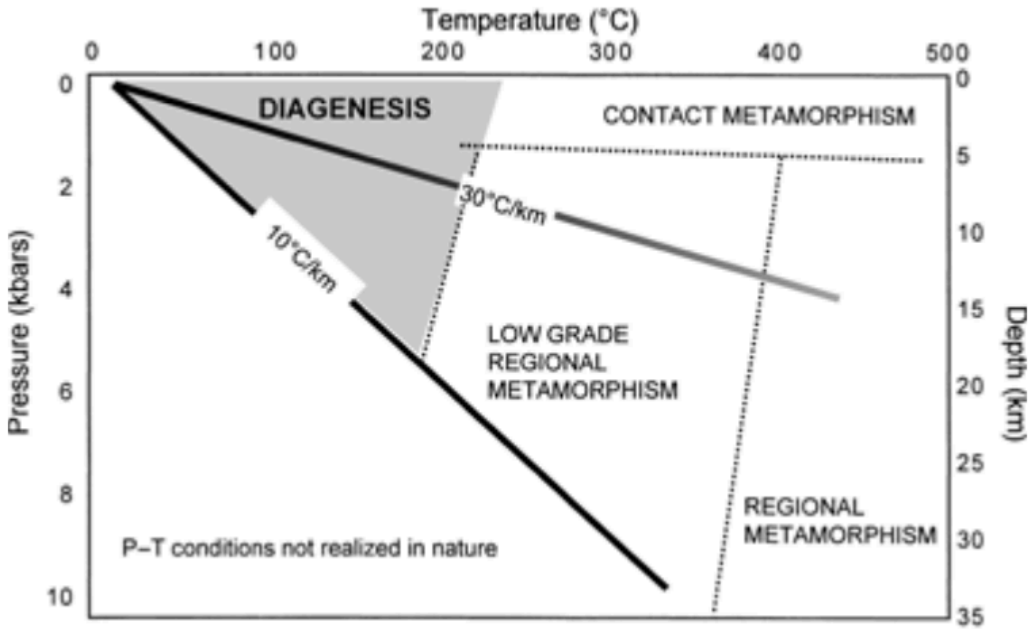

Figure 2 Shows the relationship between Diagenetic processes and metamorphism. The temperature gradients of 10°C km−1 and 30°C km−1 represents stable cratons and rifted basins respectively (Worden and Burley, 2003).

2.2 Stages of Diagenesis

The sediments undergo three different stages of diagenesis namely eogenesis, mesogenesis and telogenesis (Fig. 4). Eogenesis is the early stage of diagenesis and occurs at shallow depths, mesogenesis is represented by deep burial, and telogenesis is characterized by late stage diagenesis that represents uplift of the buried sediments (Boggs, 2006).

2.2.1 Eogenesis

Eogenesis is represented by very shallow depth, so little compaction and grain packing occur during this phase. During this phase, the meteoric water enters the subsurface, in low permeability deposits the depth of penetration is only few meters while in continental porous sandstones it may reach up to 2 kilometers (Worden and Burley, 2003).

The major diagenetic changes include bioturbation and mineralogical changes within the sediments. On the depositional surface, different organisms rework the sediments through ingesting, burrowing and crawling, and destroy the primary sedimentary structures. These processes have very little impact on the chemical composition (Boggs, 2006). The mineralogical changes during eogenesis include precipitation of minerals in marine environments e.g. pyrite glauconite, quartz overgrowths, smectite clays, carbonate cement and K-feldspar overgrowths. Eogenesis in non-marine environments represents formation of iron oxides (instead of pyrite), calcite cement, clay minerals (kaolinite) and rare quartz cement. The temperature gradient of the sedimentary basins of the world is between 20°C and 30°C and the limit of eogenesis for an average surface temperature of 10°C is 30-70°C (Boggs, 2006; Worden and Burley, 2003).

2.2.2 Mesogenesis (Burial diagenesis)

Mesogenesis is the deep burial of the sediments and major diagenetic changes are due to increase in pressure and temperature. The major changes include porosity loss by compaction and cementation. Compaction in sedimentary rocks is divided into two types, mechanical and chemical compaction. Increase in burial depth results in tighter packing of grains and loss of porosity hence resulting in mechanical compaction (Fig. 3). This type of compaction is more prominent in shallow depths (Schneider et al., 1996). Increase of depth exerts pressure on the grain boundaries and increase the solubility of grains resulting in partial dissolution of the grains. This process is known as chemical compaction.

As the burial depth increases the temperature simultaneously increases, and most of the minerals stable in the depositional environment become unstable. High temperature is favorable for the formation of denser minerals and dissolution of unstable minerals. With increasing burial depth, organic matter decomposes with release of CO_2. This CO_2 dissolves in the pore water and the pH of the pore water decreases which in turn start dissolution of carbonates. The most important chemical processes during mesogenesis are calcite and ankerite cementation, reactions of clay minerals and quartz cementation (quartz overgrowth) (Boggs, 2006).The eogenesis and mesogenesis boundary is not clear but can be explained in temperature and depth

terms Mesogenesis commonly starts in the temperature range between 30-70°C and 1 to 2 km depth (Morad et al., 2010).

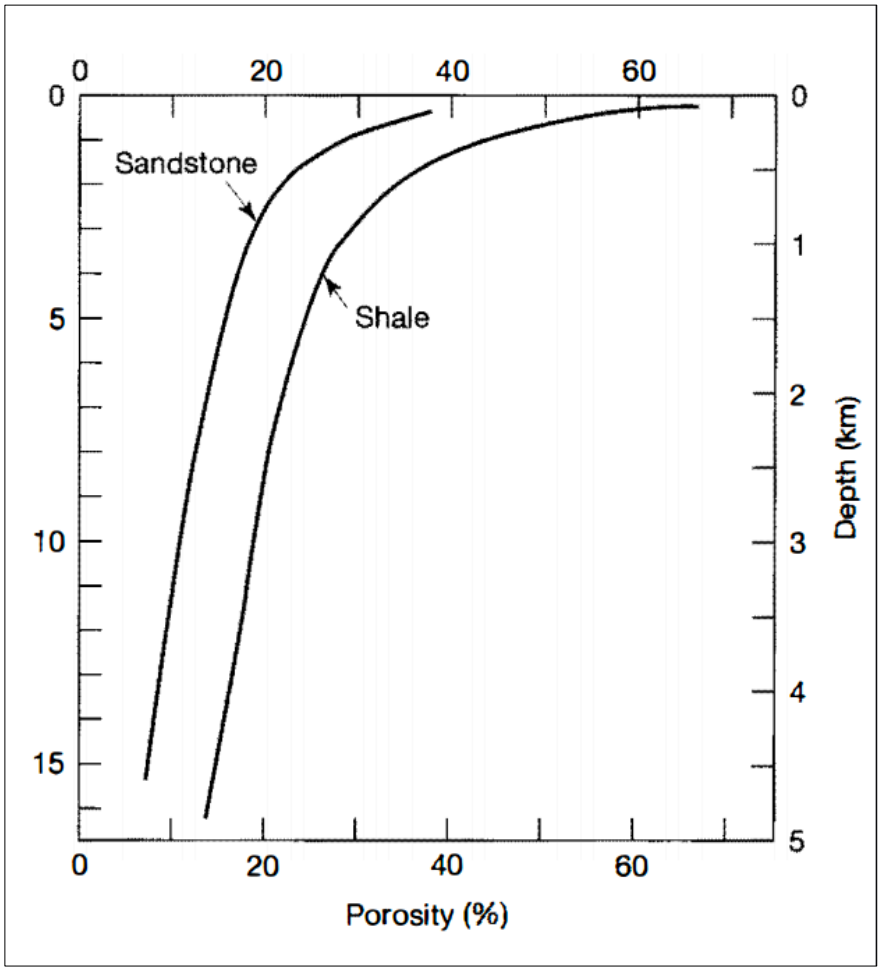

Figure 3 shows decrease of porosity with burial depth due to chemical and mechanical compaction(Boggs, 2006).

2.2.3 Telogenesis

Deeply buried rocks when uplifted and exposed react with meteoric water (surface water), resulting in mineralogical changes of the sedimentary rocks. This process is termed as telogenesis (Worden and Burley, 2003). Telogenesis is a process which brings deeply buried sediments and newly formed minerals during mesogenesis to low temperature and pressure conditions, where oxygen-rich water (meteoric) flushes out the pore water. This change in pore water may cause dissolution of previously formed minerals and cement, hence resulting in secondary porosity. Alteration of framework grains to clay minerals can also occur, and porosity is reduced (Boggs, 2006).

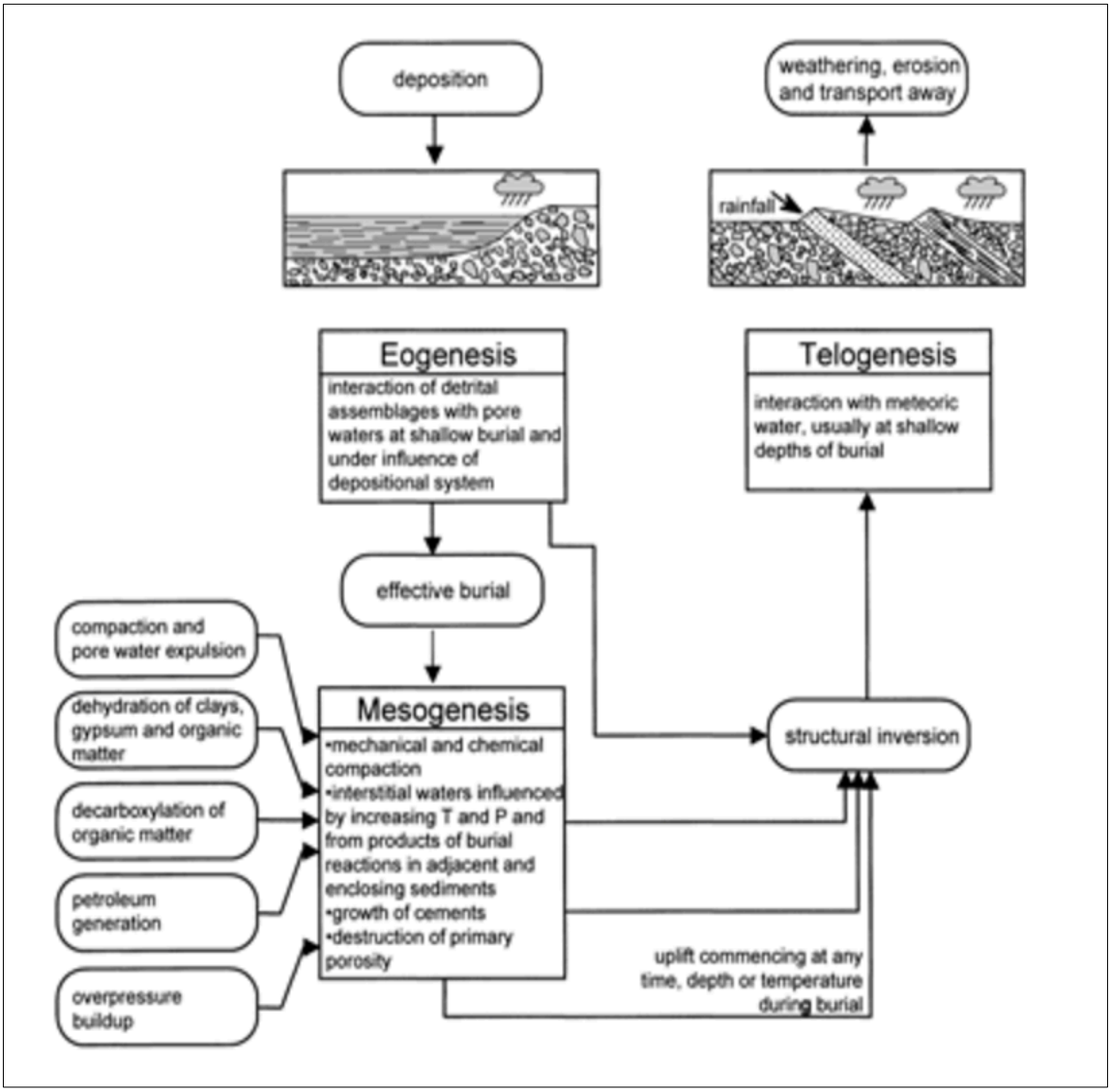

Figure 4 Flow chart diagram representing different diagenetic processes. The mesogenesis can grade on to telogenesis during any phase of burial because of uplift and erosion (Worden and Burley, 2003).

2.3 Diagenetic Cements in sandstones

The most common cements in sandstones are silica cements (quartz overgrowth, microquartz, chalcedonic quartz, opaline silica and megaquartz), carbonate cements (calcite, siderite and dolomite), aluminosilicate clay minerals, feldspar authigenesis and rarely anhydrite and gypsum (Bjorlykke, 1979; Worden and Burley, 2003).

In quartz cementation quartz overgrowth on detrital quartz grains is the most common type of cement. Silica cement precipitates in optical continuity around the quartz grain. Cements precipitated in optical continuity and not in optical continuity are termed as syntaxial and epitaxial, respectively (McBride, 1989; Worden and Burley, 2003). Siliceous fossil fragments are replaced by microcrystalline quartz. Quartz cement is mostly observed in sandstones which

are subjected to temperature around 60 to 100°C (Bjorlykke, 1979). Early quartz cementation can lead to moderate preservation of porosity due to stability of quartz against compaction.

The distribution of carbonate cement ranges from uniform to patchy distribution and can also occur in the form of concretions. When calcite precipitates, it displaces the detrital grain in a way that the detrital grain seems to be floating in the cement. Apart from pore-filling cement, carbonate cements also replace the detrital grains. Calcite cement is formed during early diagenesis and is common in litharenites, quartz arenites and arkoses (grain supported sandstones). Early calcite cementation hinders the formation of other diagenetic cements (quartz cementation and feldspar alteration) that can lead to total loss of porosity (Morad, 2009). Alteration of feldspar to kaolinite or illite and feldspar overgrowth also occur in sandstones. Si, Al, Na and K-rich alkaline pore waters is necessary for the authigenesis of feldspar. The most common clay minerals formed in sandstones are kaolinite and illite, and these cements are usually pore-filling. Kaolinite and illite formation requires acidic and alkaline pore waters respectively (Wilson, 2013).

Chapter 3 Geology of the Norwegian Sea

The Norwegian-Greenland Sea is formed because of the Cenozoic continental breakup. This Cenozoic opening of the sea resulted in the formation of Norwegian continental margin (Faleide et al., 2008). Before the Cenozoic continental breakup Greenland, Svalbard and Fennoscandia were present at the borders of a giant water body. The North Sea and Barents Sea, (shallow water seas) were once part of this giant water body. The Norwegian continental margin is divided in two types based on tectonic evolution: From 62°N to 70°N the Norwegian Sea continental shelf represent a rifted volcanic margin and from 70°N to 82°N the margin is a shear margin (Faleide et al., 2008).

3.1 Tectonic Framework and history of the Norwegian Continental Margin

The Norwegian sea continental margin is a rifted margin with a large shelf and a gentle slope. The Norwegian Sea covers most of the margin from 62°N to 69°N (Fig. 5). The Caledonian orogeny and the North Atlantic breakup are the two major tectonic episodes. Closure of the Proto-Atlantic Ocean took place during late Silurian- early Devonian time (Caledonian orogeny). Different episodes of extensional deformation occurred during the Late Devonian to Paleocene. The third and final stage of tectonic evolution is from Eocene-Present which is marked by active sea floor spreading (Blystad et al., 1995). The Møre, Vøring and Rås basins are present on the continental slope whereas the Trøndelag platform is on the coastal zone. The Halten Terrace is on the Eastern flank of these basins (Zabanbark, 2013).

Brekke et al., (1999) states that the Norwegian continental margin can be characterized into three episodes of tectonic activities since the Cretaceous;

a) During Cretaceous to Paleocene extension of lithosphere resulting in breakup.
b) In Early Eocene, late rifting with basaltic eruptions and central uplift.
c) Finally, magmatic activity together with subsidence of the continental margin.

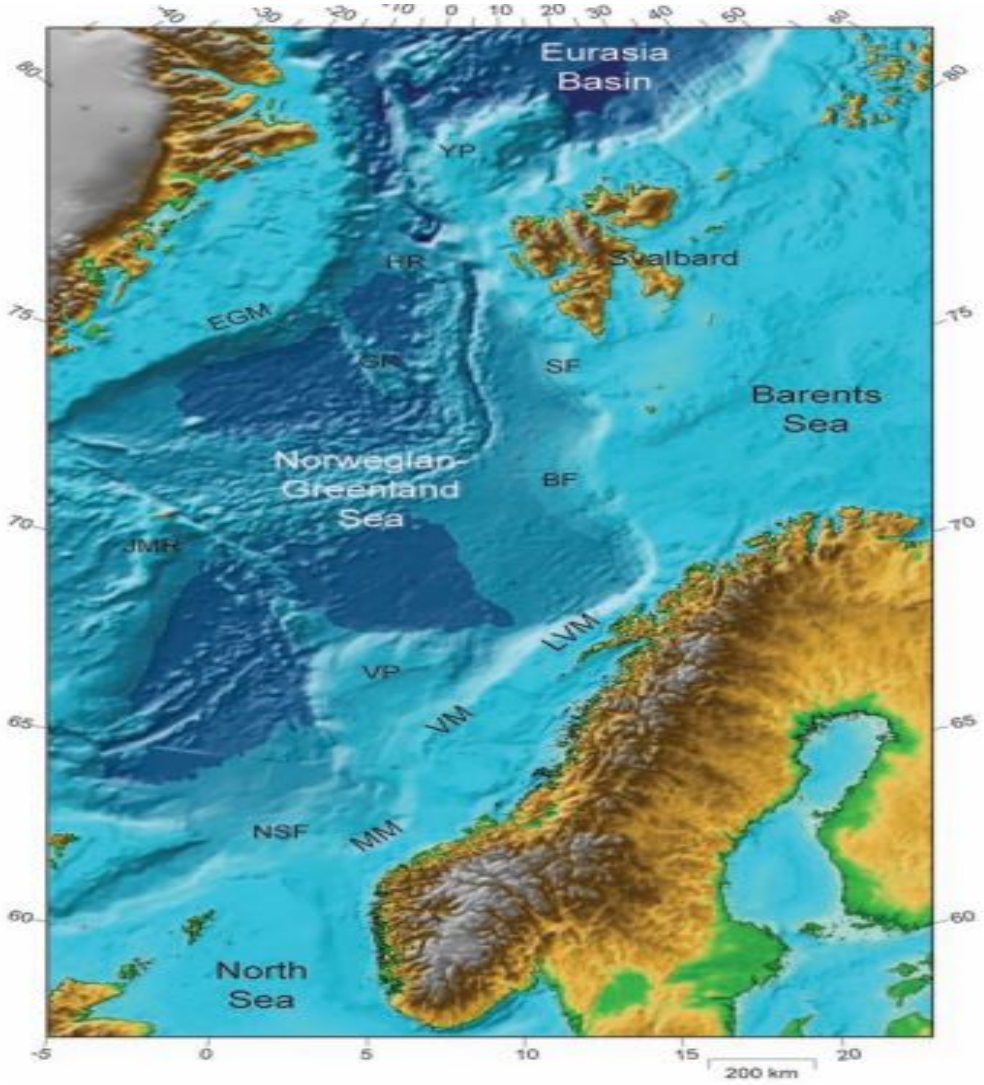

Figure 5 Regional tectonic setting of the Norwegian continental margin. YP: Yermak Plateau, GR: Greenland Ridge, JMR: Jan Mayen Ridge, MM: Møre Margin, VM: Vøring Margin, BF: Bjørnøya Fan, NSF: North Sea Fan, HR: Hovgård Ridge, VP: Vøring Plateau, LVM: Lofotebn-Vesterålen Margin, EGM: East Greenland Margin, SF: Storfjorden Fan (Faleide et al., 2008).

3.2 Structural Development

Besides the dominating, NE to SW structures of the deep basins and their flanks the continental margin is further divided by the NW-trending Bivrost and Jan Mayen Lineaments into three structural provinces.

3.2.1 The Northern structural province

The continental margin in the northern structural province is quite narrow and the main elements are the elevated areas of the Lofoten Ridge, Utrøst Ridge, Vestfjorden and Ribban

basins. The horst and grabens are formed during Mid-Cretaceous –Early Jurassic rifting, followed by rotation of grabens and uplifting and erosion of the Northern structural province. The Vestfjorden and the Ribban basins are Cretaceous half-grabens. These half-grabens are separated by the Lofoten Ridge which is a basement horst (Brekke et al., 1999).

3.2.2 The middle Structural province

In the Middle structural province, the major structural elements (Fig. 6) are the Vøring Marginal High, Vøring basin and the Trøndelag platform(Dalland et al., 1988). During Carboniferous to Late Permian the tectonic episode resulted in the formation of horst and half-graben structures in the Trøndelag Platform area. Triassic is characterized by a period of active faulting and formation of en-echelon structures. The NE-trending Froan Basin is filled with Triassic-Upper Palaeozoic sediments, and the Trøndelag Platform(central part) has been tectonically inactive since the Triassic (Brekke et al., 1999).

The Halten and Dønna terraces form the western margin of the Trøndelag Platform due to Middle Jurassic –Early Cretaceous tectonism. This margin faced intense tectonic activity which resulted in intense faulting, uplift and erosion. The Halten and Dønna terraces were separated from the Trøndelag Platform during Late Cretaceous time (Blystad et al., 1995). The Fles Fault complex (Late Jurassic- Early Cretaceous) divides the Vøring basin area. During Late Middle Jurassic-Late Cenomanian deep basin areas were formed due to crustal extension and thermal subsidence. The Halten and Dønna terraces and the depocentres of Cretaceous basins combined to form the Vøring basin *sensu stricto* (Blystad et al., 1995) during a Late Cenomanian to Early Palaeocene phase. The Early Palaeocene to Present tectonic phase is characterized by uplift of the basin area followed by erosion of intra basinal highs. Uplifting and erosion of the Vøring Marginal High occurred during Late Cretaceous-Palaeocene, followed by Palaeocene-Eocene flood basalt volcanism (Brekke et al., 1999).

3.2.3 Southern Structural Province

The major structural elements in the Southern Structural Province are the Møre Basin, Møre-Trøndelag Fault Complex and the Møre Marginal High (Blystad et al., 1995). The major tectonic phase in this province was the Jurassic-Early Cretaceous rifting episodes. In the Møre Basin there is no evidence of tectonic activity during the Cretaceous. Thermal subsidence caused the formation of basins with down-flexed flank. Møre Marginal High underwent the same tectonic phase as Vøring Marginal High (Brekke et al., 1999).

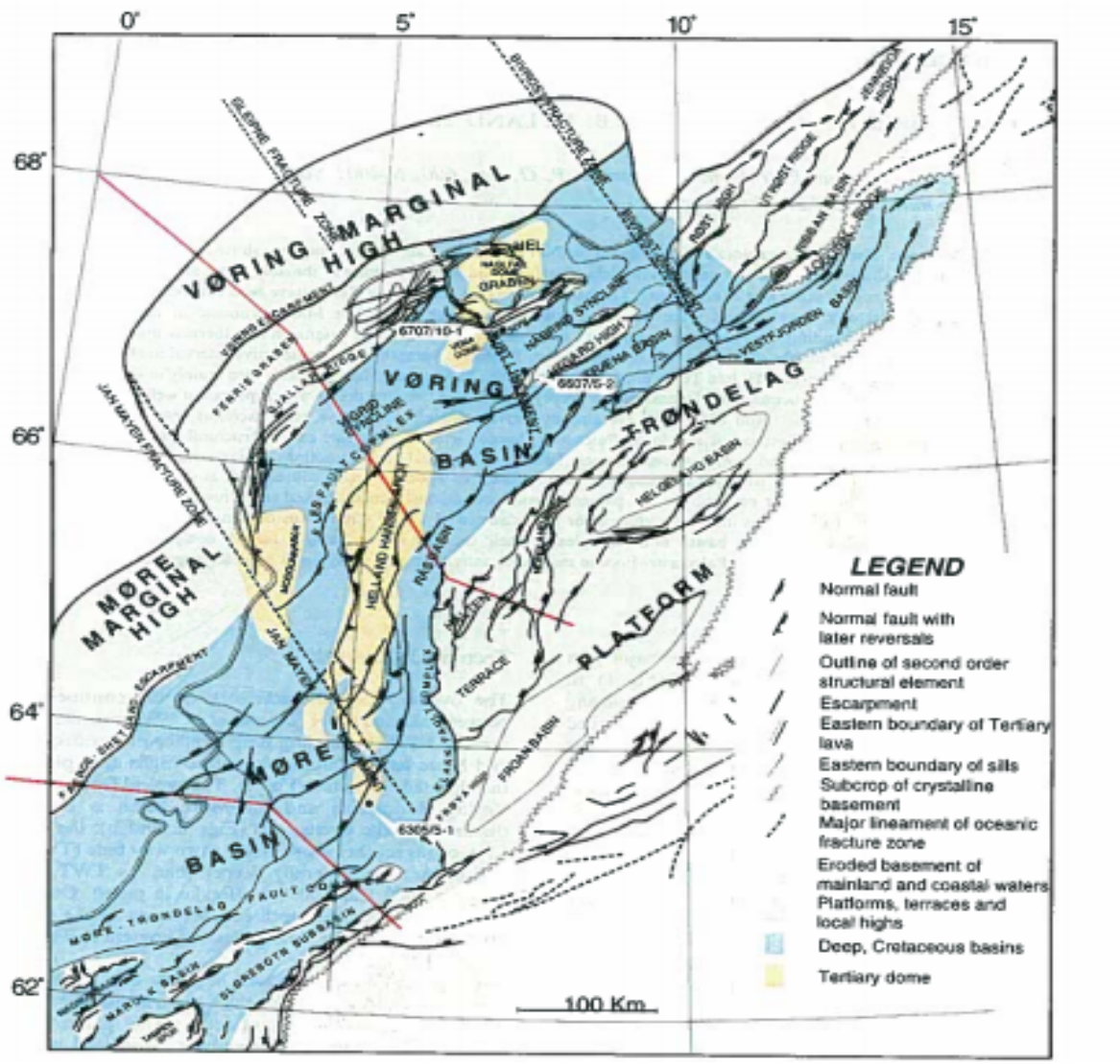

Figure 6 Major tectonic and structural elements of the Norwegian Sea continental margin (Brekke et al., 1999)

3.3 Mesozoic Sediments and Structures in the Norwegian Sea

The formation of rift basins started in Carboniferous and Permian between Greenland and Norway. The rifting continued in the Permian and Early Triassic, and as a result a bay developed southwards. The Triassic- Early Jurassic is characterized by warm climate changing to warm and humid in Late Triassic which led to extensive chemical weathering (Bøe et al., 2010; Mørk et al., 2003). Evaporites and mudstones are deposited during the Early Triassic. There was less rifting during Middle Triassic which exhibits deposition on fluvial plains (Bøe et al., 2010; Brekke, 2000). Due to renewed crustal stretching during Late Triassic marine transgressions occurred which resulted in thick deposition (⟩1000m) of mudstone and salt followed by sediments of continental origin. Deposition of coarse-grained sediments on the Norwegian

continental shelf during the latest Triassic is a result of uplifting of Main-land Norway (Müller et al., 2005).

Tidal environments were developed during the Early Jurassic and due to erosion, weathering denudation and wet climate the sediments from the mainland Norway were transported and deposited in deltas and estuaries across the coastline. Middle Jurassic reservoirs are the most important reservoirs in the Norwegian Sea (Bøe et al., 2010). NW to SE extension resulted in subsidence, and many horsts and graben structures were formed during Middle-Late Jurassic (Gabrielsen et al., 1999). Organic rich mudstones were deposited in the Mid-Norwegian shelf during Late Jurassic. In the Norwegian Sea Cretaceous is the period of rifting, and many basins (Møre, Vestfjorden) were formed. These Cretaceous basins were filled with approximately 10km sediments. The source area of these sediments is the Norwegian mainland, Nordland Ridge, and Greenland (Bøe et al., 2010).

3.4 The Trøndelag Platform

The name Trøndelag Platform was first used by Hollander, (1982) but no formal description was given. This Platform is named after Trøndelag county in central Norway. The Trøndelag Platform was formally described by Gabrielsen, (1984) and was also discussed by Aanstad, (1981). The Trøndelag Platform has an area of almost 50000 km^2 and is rhomboid in shape. The Platform is situated between 63ºN - 65º50'N and 6º20'E - 12ºE (Blystad et al., 1995). The Trøndelag Platform is the major structural element off central Norway and consists of many supplementary structural elements (Fig. 7). These elements are the Vega High, Frøya High, Helgeland Basin, Froan Basin, Nordland Ridge and Ylvingen Fault Zone (Blystad et al., 1995; Spencer, 1984).

The Trøndelag Platform in its eastern corner meets the Caledonian crystalline basement and area. On the Western part the Bremstein Fault Complex separates the Trøndelag Platform and the Halten Terrace. The south-eastern boundary is marked by the Møre-Trøndelag Fault complex. The southwestern part of the Trøndelag Platform is separated from the Jan Mayen Lineament and the Møre Basin by the Klakk Fault Complex (Blystad et al., 1995; Lundin et al., 2005).

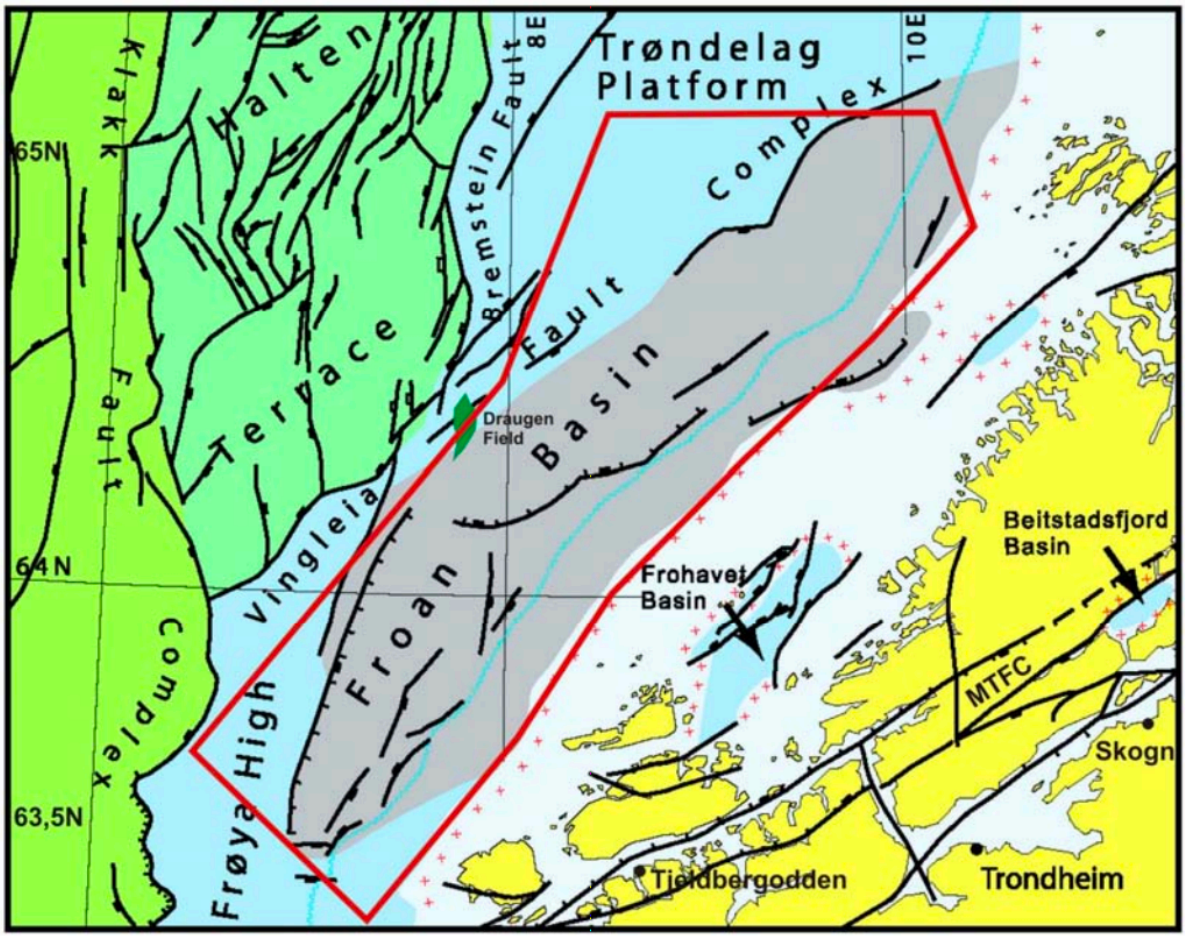

Figure 7 Geological map of Mid-Norway representing the Trøndelag Platform (Lundin et al., 2005)

3.4.1 Geology of the Trøndelag Platform

The initiation of the Trøndelag platform is marked by uplifting of the Frøya High and the Nordland Ridge during Late Middle Jurassic to Early Cretaceous. During Late Jurassic, all the uplifted areas underwent erosion and a plain was formed on the Trøndelag Platform. Further uplifting of the Nordland Ridge occurred during Cretaceous (Lundin et al., 2005). The Trøndelag Platform was tectonically active during the Middle–Late Triassic and Carboniferous-Permian times (Blystad et al., 1995).

In the Trøndelag Platform most of the faults are normal and have small displacement. These faults have NE-NNE trend. On the northern and central part of the Trøndelag Platform a Cretaceous basin (Helgeland Basin) is formed whereas on the rest of the platform either the Cretaceous strata are thin or completely absent (Blystad et al., 1995). The Jurassic and Upper Cretaceous basins are underlain by a uniform thickness of Jurassic rocks and these Jurassic

rocks are beneath the Platform surface. Pre- Jurassic rocks are deposited in a NE to SW trending en-echelon basins. An unconformity of middle Permian age differentiates between the early active faulting period and a late Triassic and Permian tectonically inactive period within these basins (Blystad et al., 1995; Lundin et al., 2005).

3.4.2 Froan Basin

The Froan Basin was defined by Gabrielsen et al. (1984) as a structural element within the Trøndelag Platform with thick Mesozoic and Tertiary sequences. Bukovics et al. (1984), and Hammar and Hjelle (1984) named this basin as Hitra Basin. The Froan Basin is named after Froan islands on the coast of Sør-Trøndelag. This basin is situated between 63º 25'N - 65º 10'N and 7º10'E - 12º12'E. The Froan Basin is 250 km in length and the width is ranging up to 50km on the northern margin. The basin is characterized by a set of half grabens with Permian to early Triassic and Late Triassic to Early Jurassic strata of approximately 3000m thickness. The Froan Basin depicts a very minor tectonic activity and only minor faults of Jurassic age can be observed. It is situated on the southernmost of many of the Permo-Triassic extensional Basins on the Trøndelag Platform (Blystad et al., 1995). During late Jurassic time fault activity took place along the Klakk Fault Complex. In the deeper parts of the basin the major faults are of Permo-Triassic age (Lundin et al., 2005).

3.4.3 Provenance of the Jurassic reservoirs in the Froan Basin

In the southern margin of the Froan Basin two shallow stratigraphic cores (6307/07-U-02, -U-03) encountered 80 meters of Upper Jurassic sandstones within the Spekk Formation. The lower 70 meters of the sandstone unit is arkosic and is Kimmeridgian to Volgian in age. The remaining upper 10 meters is subarkosic and early Volgian in age. Garnet, tourmaline, zircon and apatite are some heavy minerals within the sandstone and the unit is mostly fine to medium grained (Mørk and Johnsen, 2005). This sandstone unit indicates origin from igneous and metamorphic source rocks. The heavy minerals, feldspar rich composition and excessive microcline represents origin from a granitic plutonic rocks, while the evidence of metamorphic origin is proved by the presence of garnet (Mørk and Johnsen, 2005).

In the northern part of the Froan Basin a core (6408/12-U-01) encountered Upper-Toarcian sandstones (quartz-rich) and mudstones (kaolinite-rich) overlying weathered basement. Zircon, garnet, ilmenite and tourmaline are the heavy minerals in these northern sandstones. These deposits reflect origin from weathered basement, metamorphic and igneous rocks (Mørk and

Johnsen, 2005; Mørk et al., 2003). Figure 8 shows an interpreted seismic profile of the Froan Basin and Froya High.

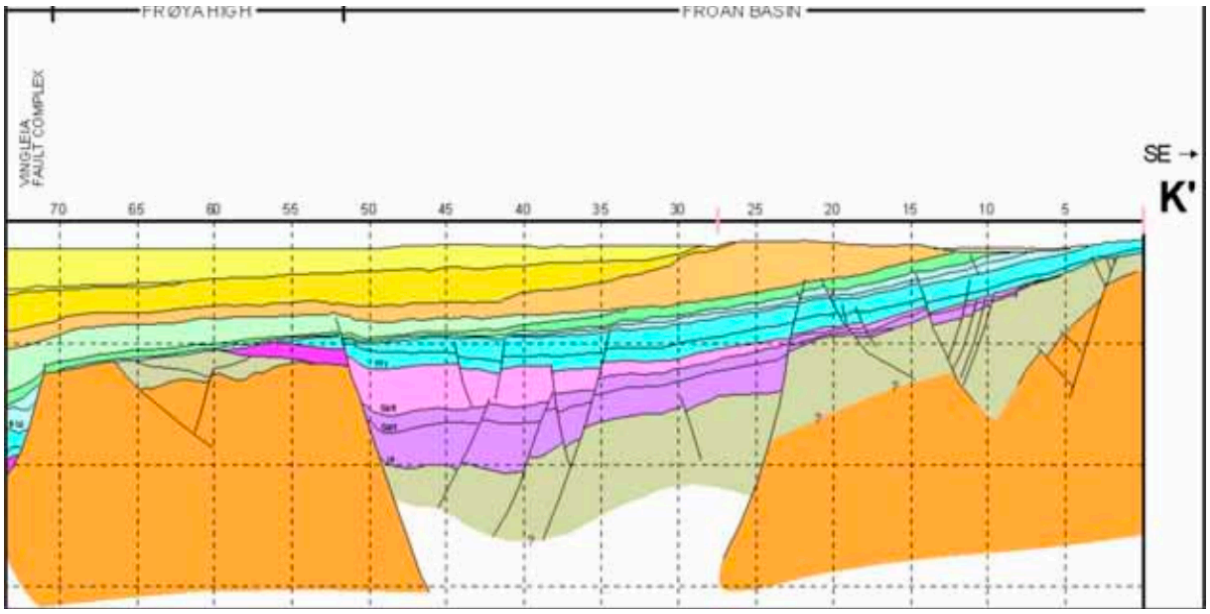

Figure 8 Interpreted seismic profile of Froan Basin and Frøya High (Lundin et al., 2005).

3.5 Lithopstratigraphy

The Permian rocks are not yet assigned any formal name or group but a 34m thick dolomitic limestone with sandstone stringers has been drilled at Rødøy High. The Permian rocks of the Norwegian Sea are correlated with rock formations in Greenland (Halland et al., 2014). The Triassic rocks are divided into two informal groups, the red beds and the grey beds. As for now the Triassic sequence is not completely drilled, but a total of 2700 m of the Triassic sequence is drilled in well 6507/6-1. Clastic sediments of continental origin corresponds to the Red beds and the Grey beds are deposited in more humid climate (Halland et al., 2014). The Lithostratigraphy scheme for the Mesozoic and Cenozoic succession is given by Dalland et al. (1984). As this Project is related to the Middle Jurassic to Lower Cretaceous (Bajocian-Berrasian) Viking Group so this will be discussed in more detail. The stratigraphic chart of the Trøndelag Platform, Halten Terrace and Vøring Basin is shown in Figure 9.

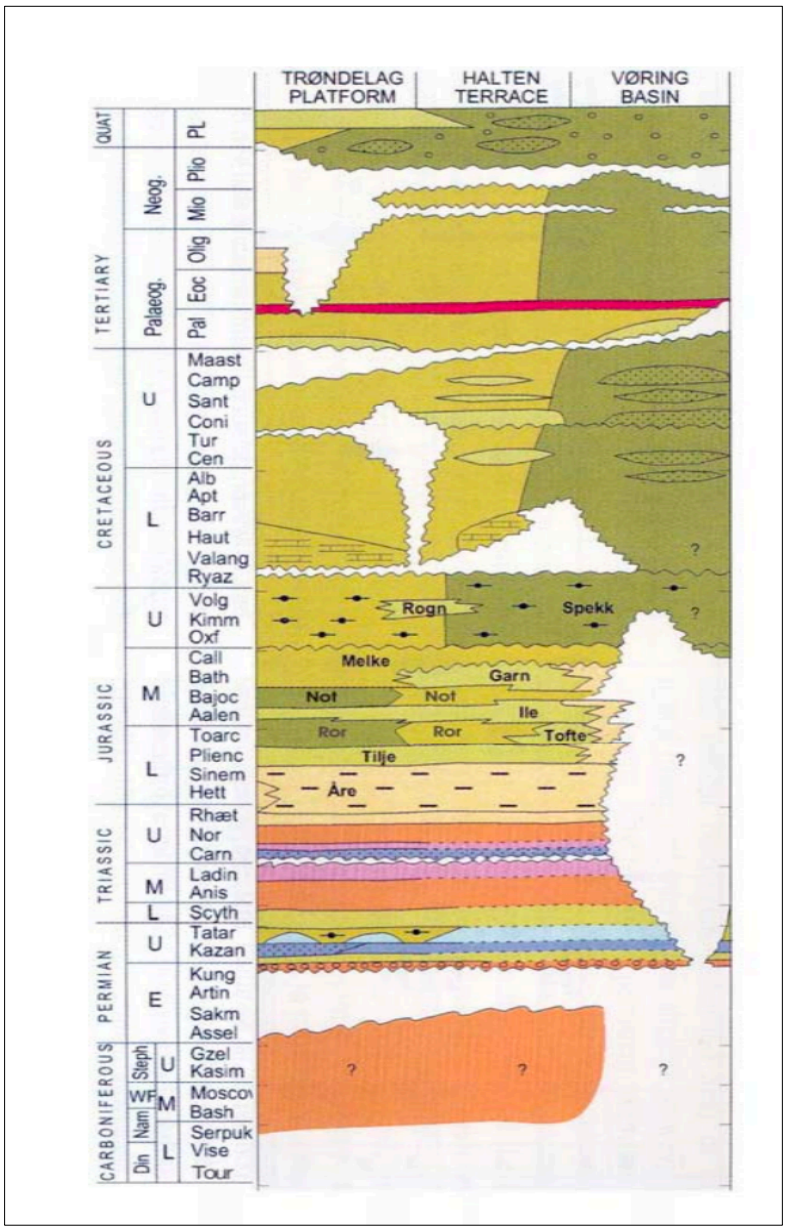

Figure 9 Stratigraphy of the Vøring Basin, Halten Terrace and Trøndelag Platform (Brekke et al., 2001).

3.5.1 Viking Group (Vikinggruppen)

This group was formally defined in the Northern North Sea by Vollset and Doré (1984). It is also defined in the Trænabanken and the Haltenbanken area. The Viking Group is widely distributed on the Trøndelag Platform and pinches out towards the Nordland Ridge (Halland et al., 2014). Seismic data from the down-faulted areas suggests a thickness of more than 1000 m. The dominant lithology of this group is mudstones and shales with a small amount of sandstone and carbonate stringers except for the Draugen Field where sandstone is the major constituent. The Viking Group is deposited in marine environment just beneath the sea floor on the eastern

margin of Trøndelag Platform (Dalland et al., 1988). The Lithostratigraphy of the Viking Group was revised by Vollset and Doré, (1984) in the North Sea and is presented in Table 1a.

Table 1 Lithology and ages of formations in the Viking Group. Data used in this table is extracted from (Dalland et al., 1988; Vollset and Doré, 1984). a) North Sea, b) Norwegian sea

(1a)

Lithostrat. unit	Age	Lithology
Intra Draupne Formation sandstone	Oxfordian-Ryazanian	Arenaceous sandstone intercalations within Draupne formation.
Draupne Formation	Oxfordian-Ryazanian	Dominant lithology is dark grey, brown to black, non-calcareous claystone with subordinate siltstone.
Sognfjord Formation	Oxfordian to Kimmeridgian/Volgian	Coarse grained, greyish brown sandstone.
Intra Heather Formation sandstone	Bathonian to Kimmeridgian	Dominant lithology is sandstone deposited with in Heather Formation.
Heather Formation	Bathonian to Kimmeridgian	Grey silty claystone with stringers of limestone.
Fensfjord Formation	Callovian	Dominant lithology is greyish brown, calcite cemented sandstone. Minor amount of shale is also deposited within this sequence.
Krossfjord Formation	Bathonian	Medium to coarse grain greyish brown sandstone with stringers of calcite cemented sandstone.

(1b)

Lithostrat. unit	Age	Lithology
Spekk Formation	Oxfordian-Ryazanian	Non-calcareous dark brown to grey mudstone.
Rogn Formation	Oxfordian-Kimmeridgian	Dominant lithology is sandstones, coarsening upward from siltstone, shale to sandstone.
Melke Formation	Bajocian-Oxfordian	Dominant lithology is claystone interbedded with limestone and siltstone. Occasional sandstone beds can also be seen.

The Viking group is divided into three formations Melke Formation, Rogn Formation and Spekk Formation in the Norwegian Sea and is represented in Table 1b.

3.5.1.1 Melke Formation (Melkeformasjonen)

Melke is a Norwegian word for soft roe or milt and this formation is compared with Heather Formation of the North Sea (Dalland et al., 1988). The Melke Formation is Bajocian-Oxfordian in age and is deposited in an open marine environment. The dominant lithology is dark grey to brown, calcareous claystone with minor siltstone stringers, but sandstone is also deposited in some parts of the Rødøy High and Dønna Terrace. On the Nordland Ridge 550 meters of Melke Formation has been drilled (Dalland et al., 1988; Halland et al., 2011).

Sharp increase in gamma ray response defines the basal contact between mudstones (Melke Formation) and underlying sandstones (Garn Formation). The Formation is widely distributed along the Haltenbanken and Trænabanken and reaches a thickness of several 100 meters (Dalland et al., 1988).

3.5.1.2 Rogn Formation (Rognformasjonen)

Rogn is a Norwegian word for hard roe or spawn. The Rogn Formation is Oxfordian-Kimmeridgian in age and is deposited as shallow marine bar deposits in the Draugen Field. These deposits are also encountered in the wells of the western part of the Froan Basin and Frøya High (Halland et al., 2014). The dominant lithology is sandstones with siltstones and shale as minor constituents. The Rogn Formation follows an overall coarsening upward trend from siltstone-sandstones (Dalland et al., 1988).

In the Draugen Field the formation has high porosity (30%), permeability (6 Darcy) and is buried at a depth of 1700 meters. The basal contact is marked by sharp and gradual decrease in sonic and gamma ray log respectively (Dalland et al., 1988; Halland et al., 2014).

3.5.1.3 Spekk Formation

Spekk is a Norwegian word used for blubber and the formation corresponds to the informally described Nesna formation (Dalland et al., 1988). The Spekk Formation is Oxfordian to Berriasian in age and the mudstones are deposited in marine anoxic bottom water conditions. The formation is deposited in the Trænabanken and Haltenbanken areas, but is locally absent over the Nordland Ridge. The dominant lithology is non-calcareous brown to greyish mudstones. The Spekk Formation has very high organic content (Dalland et al., 1988; Halland et al., 2014).

The base is marked by low sonic log reading and sharp increase in gamma ray. The Spekk Formation is time equivalent to the Hekkingen and Draupne formations in the Hammerfest Basin and North Sea respectively (Dalland et al., 1988).

The gamma ray response of Melke, Spekk and Rogn formations from two different wells is presented in Figure 10.

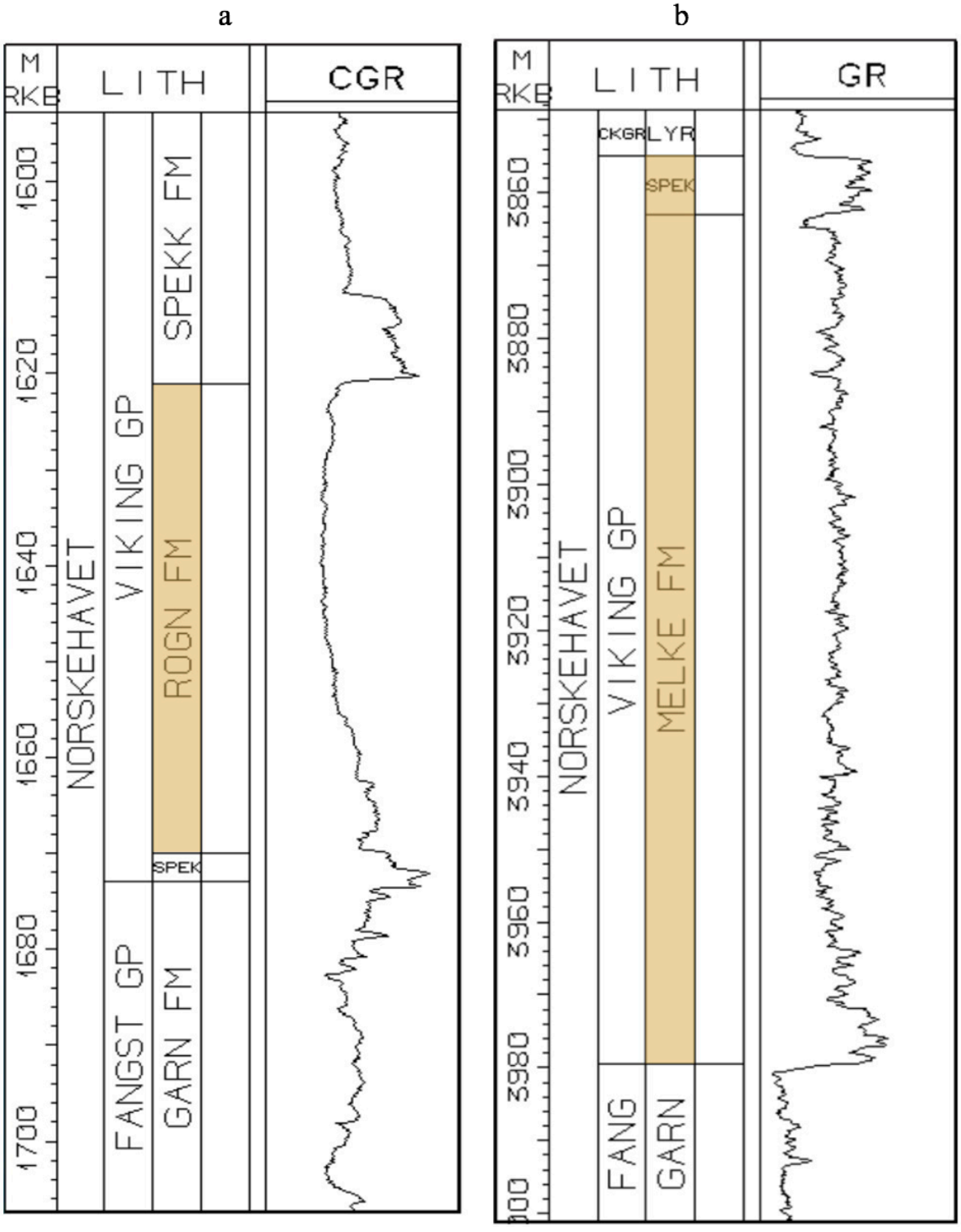

Figure 10 Shows the gamma ray response of the Spekk, Rogn and Melke formations. a) Well no:6407/9-1, b) 6506/12-4 (Halland et al., 2014)

Chapter 4 Materials and Methodology

This project is about reservoir characterization of the Rogn Formation sandstone in the Froan Basin based on the petrophysical and petrographical analysis of two shallow stratigraphic cores. 6307/07-U-02 & U-03A are the two well-logs used for petrophysical analysis, whereas thin section slides and XRD samples are used in petrographical analysis. The core photographs are used to confirm the lithology interpreted from petrophysical and petrographical analysis. The flow chart diagram of the study is presented in Figure 11.

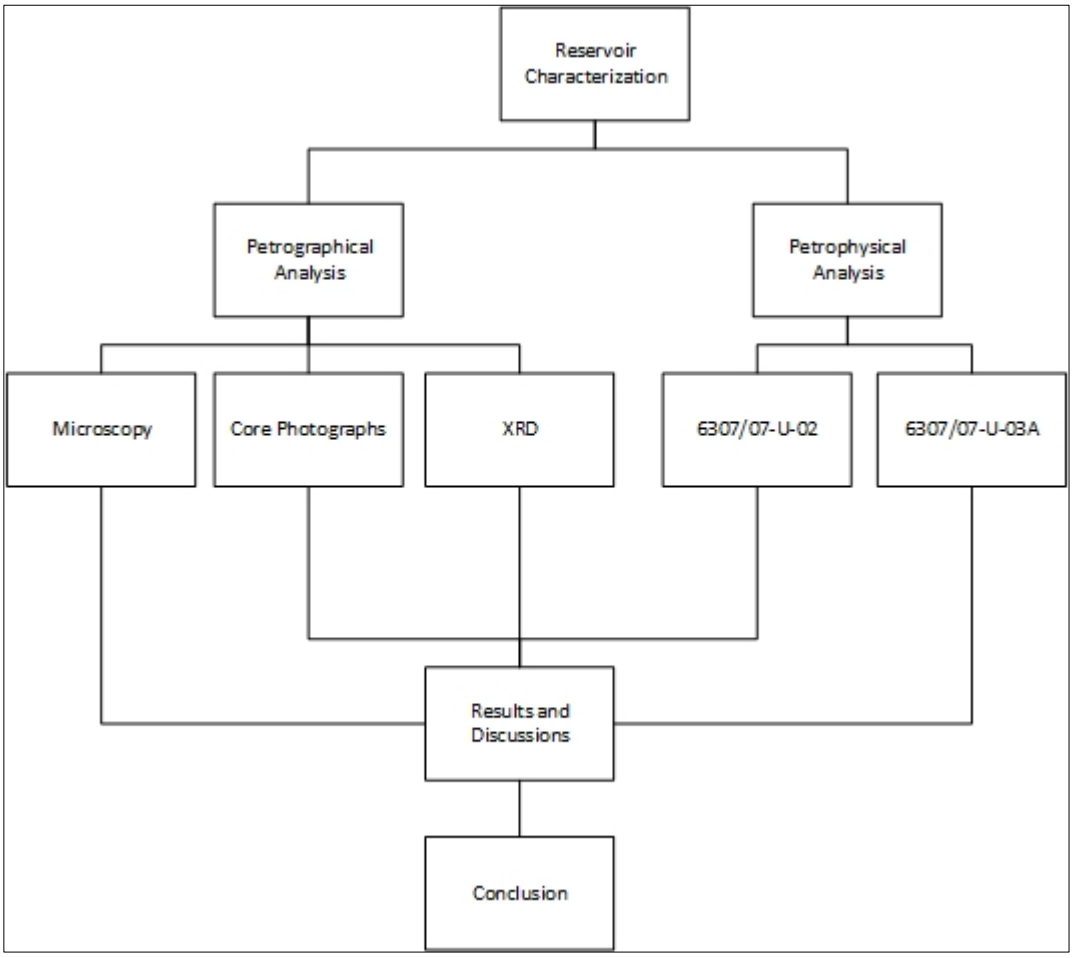

Figure 11 Flow chart diagram of the project

4.1 Petrographical Analysis

In petrophysical analysis different methods and materials are used to investigate the reservoir properties of the Rogn Formation sandstone. These include optical microscopy and XRD. Thin sections are analysed under Nikon polarizing microscope to investigate detrital grains and diagenetic features. The main objective of the petrographical analysis is to understand the

processes that are effecting the reservoir properties in the Rogn Formation sandstone. So, the focus is on diagenetic alterations, minerology, sorting, size of grains and clay minerals encountered in thin sections, as well as compaction and porosity.

4.1.1 Optical Microscopy

A total of 47 thin sections were studied from different depths of the cores. 41 samples from Core 6307/7-U-02 and 6 samples from Core 6307/7-U-03A were studied by optical light microscopy to understand the lithology, grain size, sorting, diagenetic effects and to confirm the results from the petrophysical analysis.

Modal analysis is a widely-used technique for classification and porosity measurement. The modal analysis of 9 thin sections from different depths is performed by means of a Pelcon point counter. 300 points on each sample were counted with a step length of 0.15 mm. There are some limitations to this method i.e., sometimes difficult to differentiate between quartz and feldspar, incapability of distinguishing finest grained components and inability in recognizing different fine–grained components of feldspar minerals (Hill et al., 1993).

4.1.2 Core Photographs

Core photographs of the two wells 6307/07-U-02 and U-03A are used to supplement the interpretations of lithological variation

4.1.3 X-ray Diffraction (XRD)

XRD (X-ray powder diffraction) is a method used for crystalline materials phase identification as it gives information about dimensions of the mineral's unit cell. The analysis process starts with the bombardment of X-rays on the target material and then the refracted rays are collected. There are three main components of the equipment (diffractometer) used for XRD: a) An X-ray tube, b) an X ray detector and c) a sample holder. The bombardment of high energy electrons results in the removal of inner shell electrons. When these inner shell electrons are removed Kα, Kβ (X-ray spectra) is generated. Due to the rotation of detector and target these X-ray spectra hits the target which is in powdered shape and the intensity is recorded in the form of count rate (Barbara, 2017). 5 samples from different depths are collected and results of XRD are analysed. The samples are taken from 5 different depths than the thin sections to aid the petrophysical lithology interpretation.

4.2 Petrophysical Analysis

Different geophysical logs such as Gamma Ray log, Neutron Density log, Neutron Porosity log were used in the Petrophysical analysis. The well log data is interpreted by using Techlog software. The cross-plot technique and histograms are also used to aid the interpretation. The main objectives in the petrophysical interpretation are lithology identification, porosity estimation, permeability estimation and identification of water bearing zones. The practical and industrial approach in petrophysical analysis is to use sets of different logs for interpretation because every single geophysical log contains certain limitations and uncertainties. These uncertainties can affect interpretation therefore always rely on set of logs for Petrophysical interpretation. Different logs used here in lithology, porosity and permeability estimation are discussed below.

4.2.1 Lithology Identification

In a sedimentary basin, the major lithology's are shales and sandstones. The gamma ray log is widely used and is a useful log to differentiate between shales and sandstones. The gamma ray log measures the natural radioactivity of the sediments. The natural radioactive elements are uranium, thorium and potassium. Shales contain significant amounts of uranium and therefore the gamma ray log shows higher value in shales. On the other hand, the major minerals in sandstone are quartz, feldspar and rock fragments. Absence of radioactive elements in sandstone results in low gamma ray signature in clean sandstones. The presence of heavy minerals with radioactive elements and presence of potassium-feldspar can give high gamma ray signature because of radioactive nature of potassium. In such case the neutron-density crossover is additionally used with the gamma ray log to differentiate between lithology.

The Caliper log can also be used along with gamma ray log and neutron-density crossover to help the lithology interpretation. The shales are soft in nature and cause caving in bore hole. The caving in the shales will higher the reading of the Caliper log. In case of sandstone the Caliper gives lower reading because of formation of mudcake in the sandstones. Sandstones are porous and permeable therefore the drilling mud particles penetrate porous sandstone and cause formation of mudcake along bore hole wall.

4.2.2 Porosity and Permeability estimation

In Petrophysical analysis different logs are used to calculate porosity in zones of interest. Different estimated porosities logs in petrophysical analysis are neutron porosity log (NPHI),

density porosity log, sonic porosity log. The porosity estimated from geophysical logs is not true in most cases because of the limitation of each log. The neutron porosity log measures porosity based on presence of hydrogen in the rock formation. The hydrogen is present in water or hydrocarbons that are filling pore spaces, therefore the porosity is calculated as a function of the hydrogen index (HI). In case of shales the water is present in the structure of clay minerals, and in turn hydrogen is present, therefore the neutron porosity log overestimates porosity in shales. The neutron porosity log only gives accurate values in water-saturated limestone. This overestimation of porosity by neutron log in shales is called shale effect. Another uncertainty associated with the neutron porosity log is the gas effect. If gas is present in pore spaces of sandstone, then the neutron log underestimates porosity because gas contains less amount of hydrogen as compared to oil (Pechnig et al., 1997).

The density porosity is measured based on rock bulk density. The rock is bombarded with alpha particles and the return of alpha particles is counted on the sensor in density log tool. The density of the rock depends on the minerals forming the rock matrix and fluids occupying the pore spaces. Gas is less dense as compared to oil and water, therefore the presence of gas can underestimate porosity from the density log.

The most authentic porosity is the porosity calculated from core samples by using laboratory techniques. In absence of core samples the industrial approach is use of average porosity. The average porosity of neutron-porosity and density-porosity logs is mostly used in petrophysical analysis. In this study, the density porosity is used for interpretation. The log data are calibrated by using core data, i.e. the red dots in Figure (12) are representing core porosity and permeability.

For permeability estimation, linear relationship of core porosity-permeability is developed using the following equation:

$$Y = 9.192E - 05e^{0.49347x} \quad (1)$$

where y is the permeability, and porosity is denoted by x.

Chapter 5 Results

In this chapter, the results of the petrophysical and petrographical analysis are presented. The first sub chapter represents the petrophysical interpretation of the two studied wells. The logs are divided into different zones and each zone is explained in detail. The Petrographical techniques and their respective results are presented in the second sub chapter.

5.1 Results Petrophysical Analysis

Geophysical data from wells 6307/07-U-02 & U-03A is used in this project to investigate lithology, porosity and permeability of the Jurassic rocks encountered in the Froan Basin. Well 6307/07-U-02 contains calliper, gamma ray, neutron density, sonic porosity, density porosity, density and corrected permeability (klinkenberg effect) logs. The well 6307/07-U-03A contains calliper, gamma ray, sonic log, sonic porosity and corrected permeability logs.

5.1.1 Well 6307/07-U-02

The well 6307/07-U-02 is divided into 10 different zones and each zone is discussed in detail. The interpreted petrophysical log of this well is given in Figure 12. The zones were categorized by monitoring the changes in different log properties. Each log was analyzed separately and then the region having the same properties were combined to form the zone. Properties such as Gamma Rays, density porosities and permeability's were evaluated and based on that classification was done. The results and availability of XRd and thin sections data in the respected zones of this well is presented in Table 2.

5.1.1.1 Zone 1

This zone is represented by low gamma ray log values approximately 40 API. There is positive separation in neutron-density log and low sonic log values. No core data is available for this zone. Based on neutron density cross plot, very low permeability values (0.1 milli Darcy) and high gamma ray this zone is defined as shale.

5.1.1.2 Zone 2

The zone 2 is characterized by high gamma ray of approximately 105 API. Neutron-density log shows a positive separation, permeability is moderate and sonic log values are high. No core data for porosity and permeability is available. The neutron-density log shows decrease in neutron-porosity and density, so this zone is interpreted as shale and average porosity in this

zone is 16%. The average permeability calculated in this zone is 5 milli Darcy. The cross plot is also indicating that the zone 2 is shale, as the zone lies towards the right side (Figure 13).

Table 2 The results of the petrophysical analysis and availability of thin sections and XRD data

Zone	Depth (m)	Lithology	Porosity (%)	Permeability (milli Darcy)	XRD	No of Thin sections
Zone1	0-17	Shale	5	0.1	-	1
Zone2	17-27.50	Shale	16	5	-	-
Zone3	27.50-43	Shale	13	5	-	-
Zone4	43-85	Shale	25	50	-	1
Zone5	85-100	Shale	25	10	Yes	1
Zone6	100-105.40	Shaly sand	20	5	Yes	-
Zone7	105.40-117.86	Sandstone	18	10	-	7
Zone8	117.86-126	Sandstone	25	5	-	3
Zone9	126-179.65	Sandstone	30	330	Yes	23
Zone 10	179.65-185	-	-	-	-	5

5.1.1.3 Zone 3

Zone 3 shows increase in gamma ray approximately150 API. Positive separation in neutron-density log is less and sonic log porosity is stable averaging 20%. In this zone density-porosity is fluctuating and averaging around 15% and permeability is 5 milli Darcy. The caliper log is stable showing in gauge hole. This zone is also described as shale. The organic-rich shale (Spekk Formation) is overlain by the Lange Formation at approximately 35 m depth in core 6307/07-U-02 (Langrock and Stein, 2004) which confirms the interpretation.

5.1.1.4 ZONE 4

Gamma ray values in zone 4 are high and averaging approximately 300 API. The calibre log suggests that the hole size is stable. Neutron porosity is increased (45%) and that can be due to increase in shale content. ¨ So, based on above mentioned observations this zone is defined as shale.

5.1.1.5 Zone 5

Zone 5 represents high gamma ray values around 300 API. Positive separation between neutron-porosity logs is same as in zone 4. The sonic log shows a constant value of 300-450μs/ft. The density porosity and permeability values are 22% and 10 mDarcy respectively. This zone is interpreted as shale.

5.1.1.6 Zone 6

In this zone caliper log shows that the hole is stable and in gauge. High gamma ray values around 250 API are noted in zone 6. The neutron porosity is 45% and density is 2.2 g/cc in this zone. The sonic porosity and density porosity 20 and 22% respectively. An increase in permeability is noted in this zone and is interpreted as shaly-sand.

5.1.1.7 Zone 7

Zone 7 is characterized by low gamma ray, decreasing neutron-porosity (30%)and density 2.35 g/cc. Sonic porosity in this zone is around 18% and density total porosity is 22%. The caliper log is same as in zone 6 and sonic transit time is 38μs/ft. The separation in neutron-density log is positive but is decreasing which suggests that we are approaching the water zone. This zone is defined as sandstone. The gamma ray in this zone is high but as confirmed from thin sections and XRD the sandstone contains K-feldspar and clay minerals.

5.1.1.8 Zone 8

In zone 8 neutron-porosity, density, sonic and permeability logs have same values but this zone shows an increase in gamma ray values. The gamma ray is approximately 200 API because the sandstone contains feldspar and clay minerals (kaolinite). This zone is also interpreted as sandstone.

5.1.1.9 Zone 9

Zone 9 is the water zone and is represented by high gamma ray, small positive separation and in gauge hole. The neutron-porosity, density-porosity and sonic porosity all have the values of approximately 30%. The density value within this zone is approximately 2.2g/cc and is a high permeability zone. This zone is interpreted as sandstone.

5.1.1.10 Zone 10

In zone 10 core data is available but there is no log data so it is impossible to make any interpretations on the lithology of that zone.

In summary density porosity is used during this study which is obtained at different depths in a zone and then average of these porosities is the representative of each zone. Permeability is calculated using the same procedure and the unit is milli-Darcy. Porosity and permeability values for zone 10 cannot be calculated due to lack of data. Minor difference in core porosity/permeability and the results obtained from the log is observed. If further investigation is required it is recommended to use core porosity depending on the availability, else this extracted data can be used. Based on petrophysical analysis Zone 9 represents excellent reservoir properties.

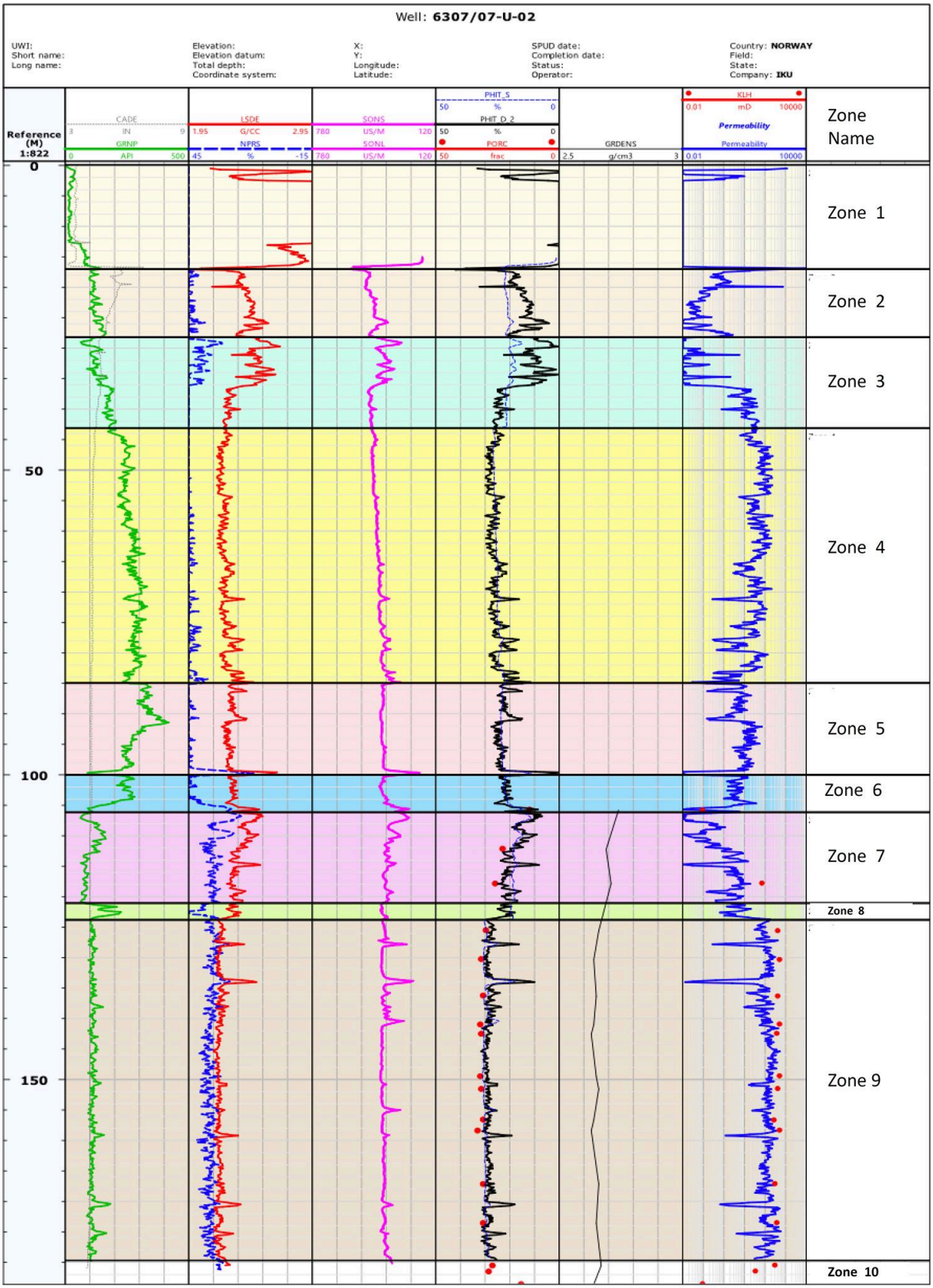

Figure 12 Interpreted Petrophysical log of well 6307/07-U-02. The red dots are the core porosity and permeability value. GR (green), Caliper log (grey), Neutron Porosity log (blue), Density log (red), Sonic log (pink), Density porosity (black), Permeability, blue and red dots represent the core data.

5.1.2 Neutron Density Cross plot and Grain-density histogram

The Neutron density crossplot is an excellent tool to differentiate between lithology and estimate porosity. The crossplot contains bulk density on y-axis and neutron porosity on x-axis. The model lines in the crossplot explain the type of lithology and porosity. The uppermost model line represents pure quartz sand. The area below the model lines represent the shales. It is of great importance which model is chosen to interpret lithology. The selection of the model lines depends on the rock matrix. If the model is designed by using the matrix input for shaly sand it will not interpret the data correctly because shaly sand does not always contain only mineral quartz and clay. Other minerals like feldspar are also present and must be considered. The most general crossplot model for complex lithology gives better estimation. In this study, the general model for complex lithology is used for interpretation (Fig 13).

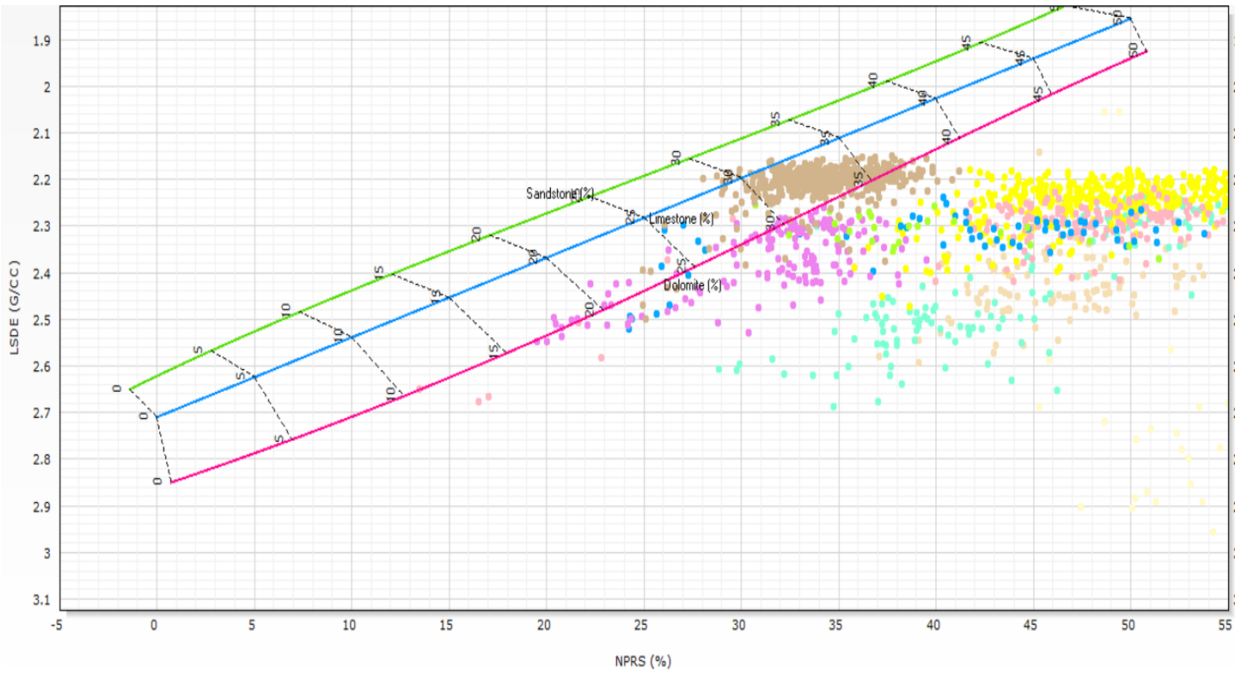

Figure 13 Neutron-density crossplot and of well 6307/07-U-02. Where Neutron porosity is on x-axis and Density porosity on y-axis.

In Figure 13, the crossplot of neutron-density from well 6307/07- U-02 is shown. Most of the data points in the crossplot are falling below the model lines and in the shales area of the crossplot. The top few meters of the well shows very low GR value which possibly is the sandstone, but in this section neutron log is not available and therefore crossplot of neutron-density is not useful in this section of the well. In Figure 13 the data points falling in-between model lines are possibly sandstone, that is interpreted earlier from the GR log. This interpretation could contain errors and uncertainties because the most generalized model is

used, however the results from neutron-density crossplot are showing good agreement with the interpretation made from the GR log.

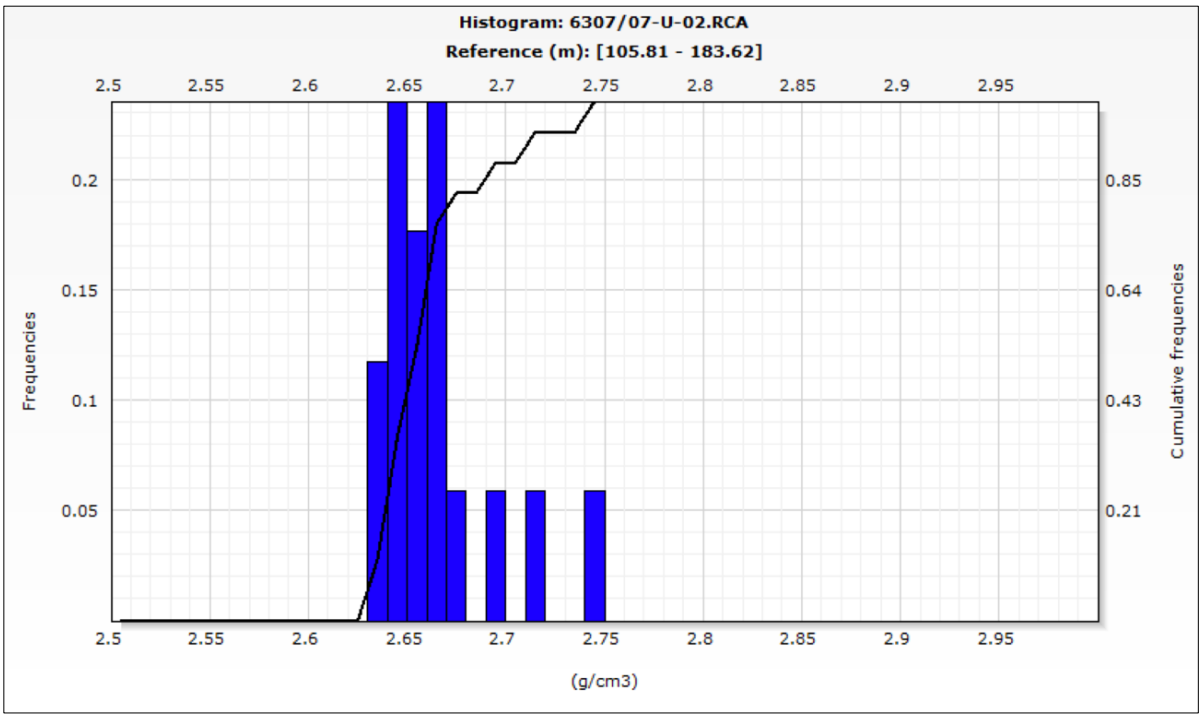

Figure 14 Grain-density histogram of well 6307/07-U-02

The histogram in Figure 14 shows the distribution of grain density. The grain density values are represented on x-axis and frequency values are on y-axis. The mean value for grain density is 2.66 g/cm^3 in the studied samples (Fig. 14), and this grain density is used to calculate the density porosity.

5.1.3 Crossplot of Porosity-permeability

Linear relationship between core porosity and core permeability is developed to calculate log permeability from log porosity (Fig 15). The relationship between core porosity and permeability is developed using Equation 1. This relationship is not perfect due to the deviation of core permeability from log permeability (Fig. 12).

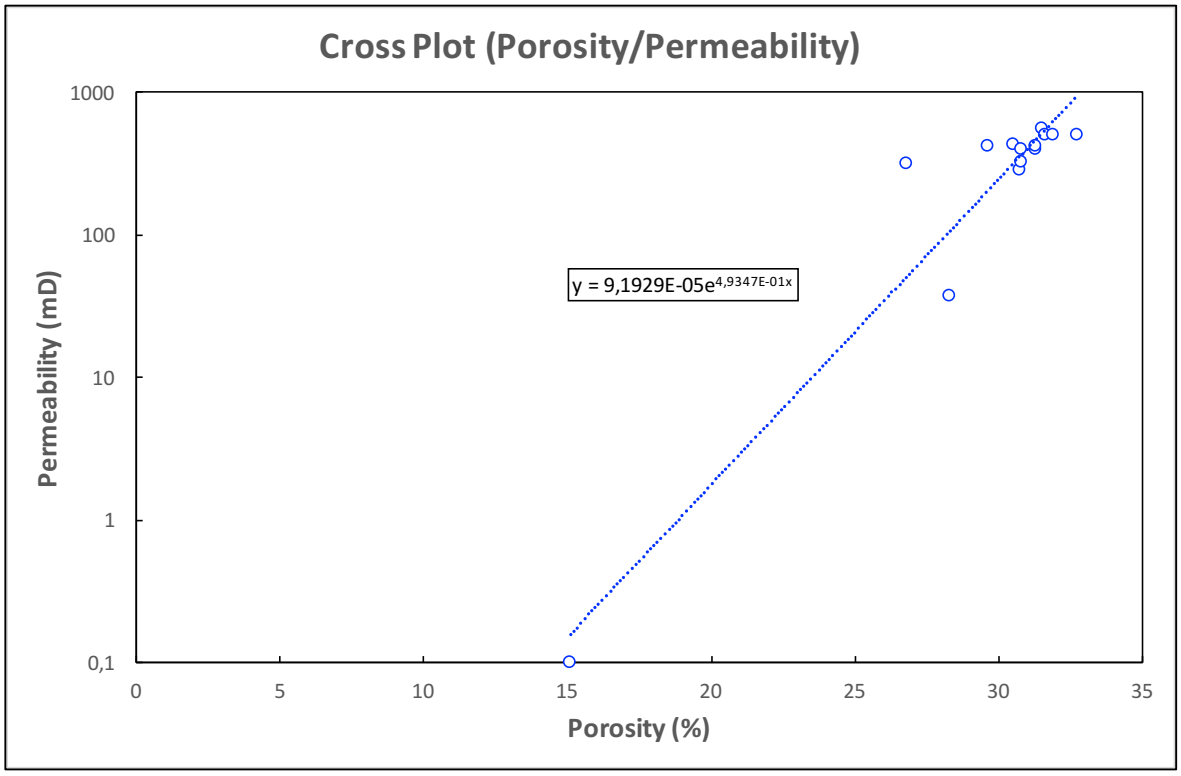

Figure 15 Porosity/permeability cross-plot

5.1.4 Well 6307/07-U-03A

This well is divided into 4 different zones but due to limitations of log data, attempts are only made to describe the lithology. The core data are available only for upper 18 meters of the core and in that zone the petrophysical data is not available. The interpreted petrophysical log of well 6307/07-U-03A is shown in Figure 16. The results and availability of XRD and thin sections data in the respected zones of this well is presented in Table 3.

5.1.4.1 Zone 1

Zone 1 is represented by low gamma ray values and stable caliper log. No other information is available to predict the lithology so on the information available this zone is interpreted as sandstone.

5.1.4.2 Zone 2

The gamma ray is around 77 API and the caliper log is stable indicating a smooth drill. The gamma ray is showing high values that prove the presence of shale content in the sandstones.

5.1.4.3 Zone 3

In zone 3 the hole is again stable having a high gamma ray signal of around 120 API. Based on available data this zone is interpreted as shaly sand. As there is no other log available for this zone the lithology interpretation cannot be confirmed in petrophysical analysis.

5.1.4.4 Zone 4

In zone 4 the gamma ray values are around 160 API. The drill hole size has increased compared with previous zone indicating washout or caving. The sonic porosity is around 30% and this zone is showing high permeability which may suggest sandstone, but since no other log is available such as neutron-density cross plot it cannot be further investigated.

Table 3 Zones and lithology of well 6307/07-U-03A and availability of XRD and thin section data.

Zone	Depth (m)	Lithology	XRD	No of thin sections
Zone1	0-6	sandstone	-	-
Zone2	6-19-19.30	sandstone	Yes	2
Zone3	19.30-24.90	shaly sand	-	2
Zone4	24.90- 75	sandstone	Yes	2

The porosity interpreted from different zones in petrophysical analysis is cross checked with core photographs and confirms the interpretation.

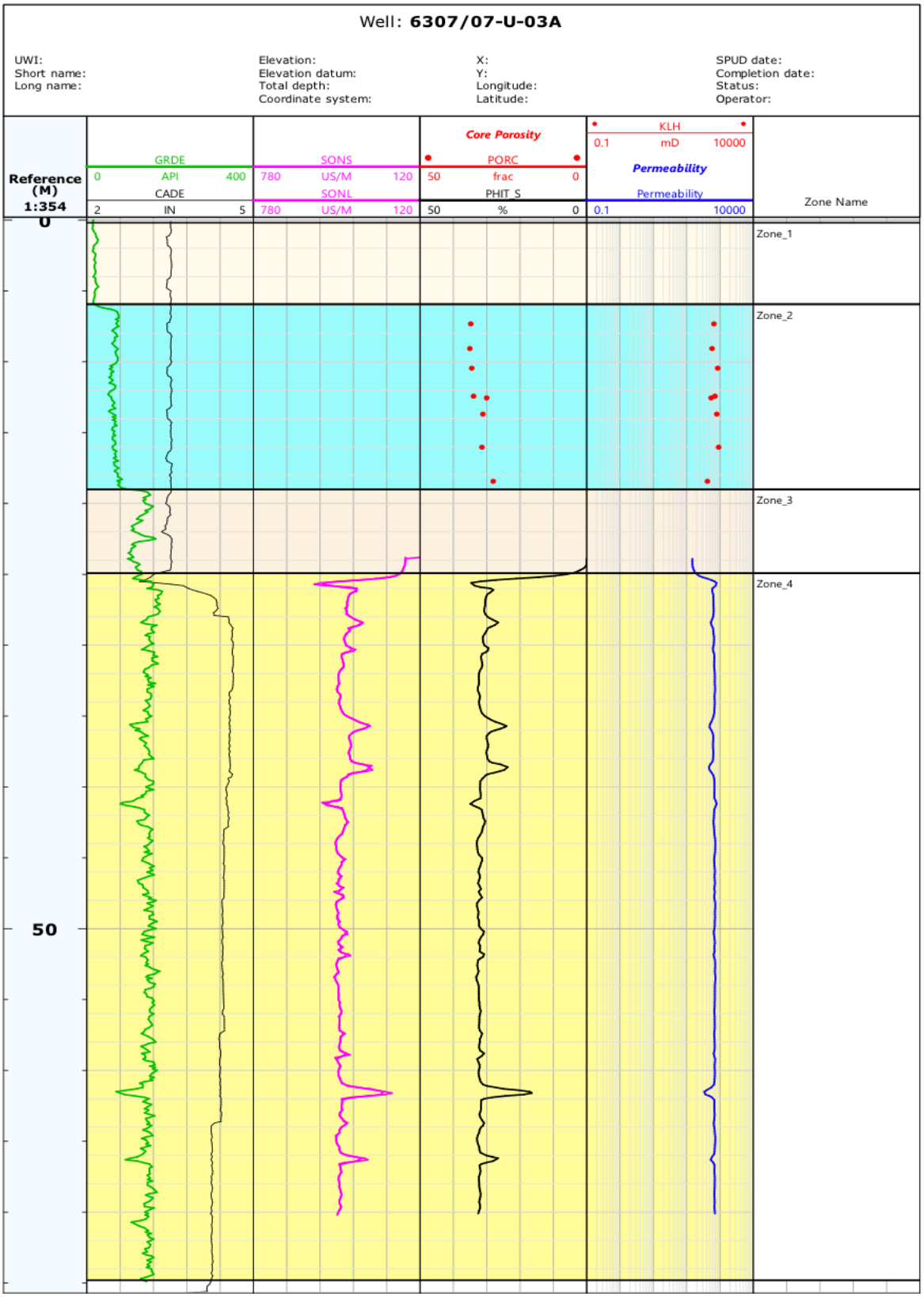

Figure 16 Interpreted petrophysical log of well 6307/07-U-03A. The red dots are representing the core data. Red dots represent the core data.

5.2 Results Petrographical Analysis

In this section, the results of the three methods used in petrographical analysis are given. As sometimes under optical microscope it is difficult to distinguish between different kinds of feldspar and fine clay minerals so the XRD results are used to calibrate the results. 9 thin sections were point counted for better understanding of the mineralogical composition and the results are presented in Table 5.

5.2.1 Microscopy Results

47 thin section samples from the wells 6307/07-U-02 and U-03A have been studied to investigate the diagenetic alterations and mineralogy of the Rogn Formation Sandstone Table (4). The Upper Jurassic sandstones (Rogn Formation) encountered in the cores is confined within the shales of the Spekk Formation. In the well 6307/07-U-02 a total of 78 meters of sandstone is cored. Based on compositional variation, this Rogn Formation sandstone is divided into two subunits. The upper sub unit is from 105.81 meters to 117 meters, and the lower sub unit is from 117-183 meters. The lower sub unit is fine-medium grained and the composition differs from the overlying upper sub unit by its higher microcline content, less lithic fragments and lower mica content. Biotite, chlorite, glauconite and some heavy minerals are also encountered in the lower subunit. The zircon encountered in the thin sections is euhedral to subhedral in shape. Rock fragments of quartzite and feldspar are also present. The grains in this subunit are sub rounded-sub angular in shape. These sandstones show intergranular and intragranular porosity, the major porosity reducing factor is mainly pore-filling clays, and calcite cement (Fig. 17). Minor chlorite and glauconite also occur as cement. Kaolinite is abundant clay mineral that is resulting in the loss of porosity

The upper unit is approximately 12 meters in thickness and consists of fine-coarse grained sandstone. The detrital composition of the upper unit is quartz, feldspar, high mica content, lithic fragments and occasionally glauconite. Accessory heavy minerals i.e. zircon is also observed in the upper sub unit. The grains in this subunit are sub rounded-sub angular in shape and well-moderately (occasionally poor) sorted. These sandstones show intergranular porosity, the major porosity reducing factor is pore-filling clays, carbonate cement and mechanical compaction.

The major porosity type is primary porosity, but some secondary porosity is also developed due to the alteration and dissolution of feldspar (Fig. 18). Bending of mica is also seen in the samples (Figure 19). Feldspar over growth is also observed in the thin sections. Few beds of the lower sub unit show moderate to poor sorting and the grains are angular in shape. The

sandstones encountered in well (6307/07-U-03A) are also arkosic. The shales deposited on the top and bottom of the sandstones are organic rich, and contains fine grained detrital grains of quartz and feldspar. The arkosic sandstones represent a general coarsening upward sequence from zone 9-7.

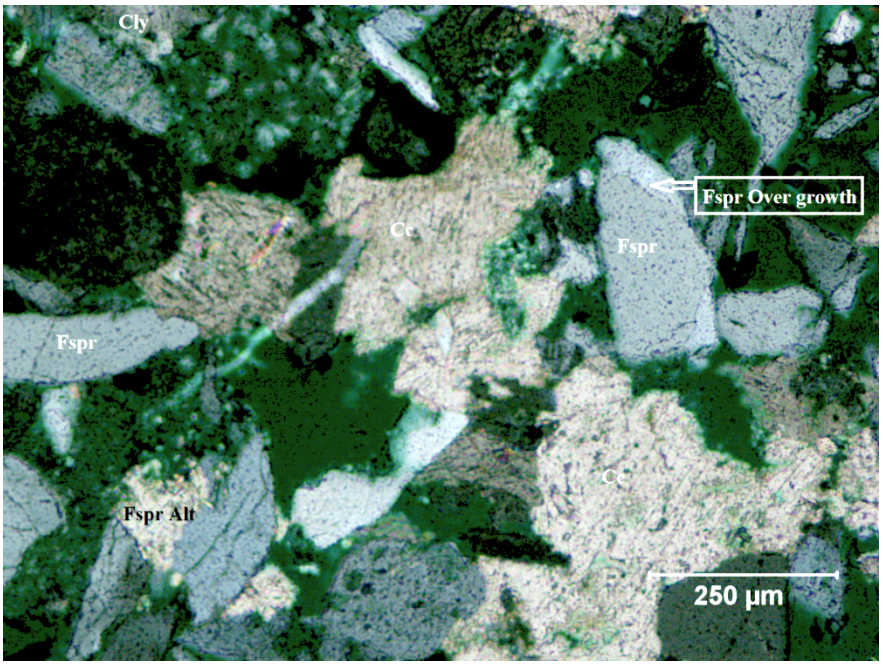

Figure 17 Cross polars, optical micrograph image from 15.34 m. Major porosity resducing elements in the Rogn Formation sandstone. Cc: Calcite cement, Cly: Clay minerals.

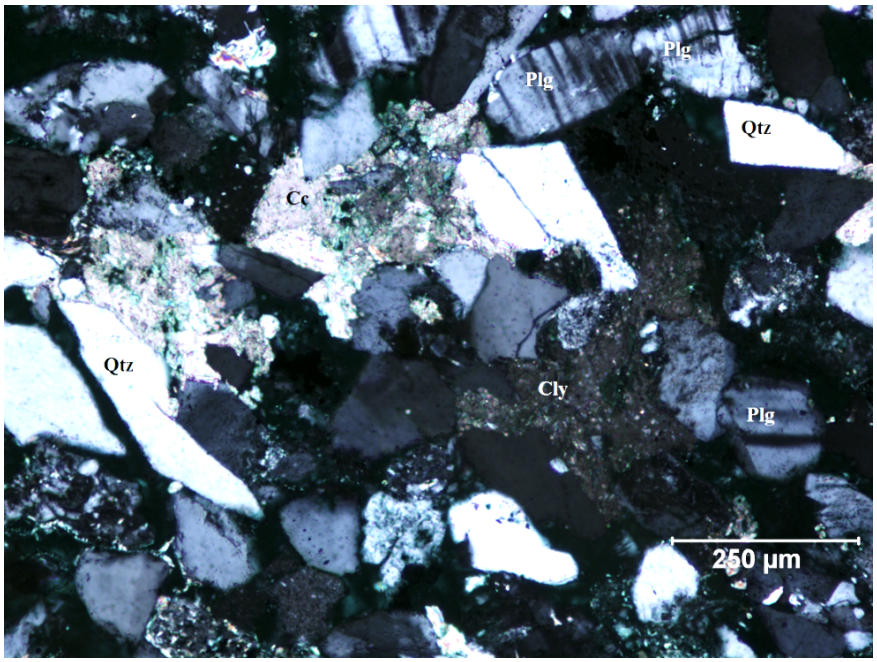

Figure 18 Cross polars, optical micrograph image from 129.50 m. Arkosic sandstone showing dissoloution of feldspar and precipitation of kaolinite/calcite cement in the secondary pores. Plg: Plageoclase, Cly: Clay minerals, Qtz: quartz.

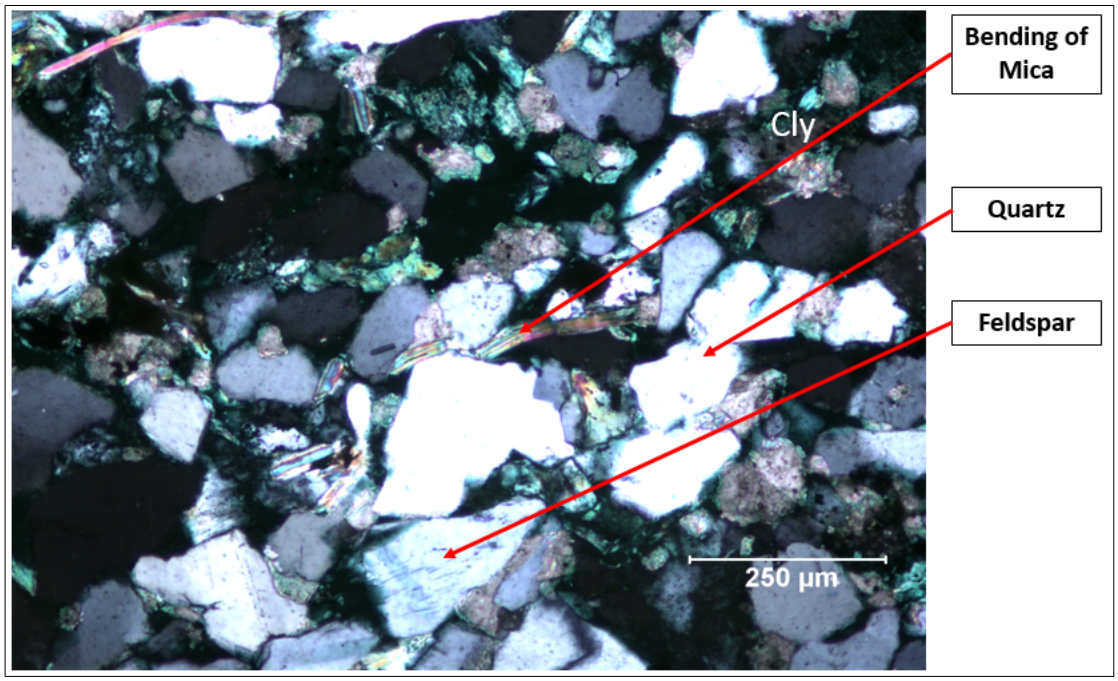

Figure 19 Cross polars, (Optical micrograph image from 181.55m. Arkosic sandstone showing compaction (mica bending) and high inter granular volume.

Table 4 Description of thin section slides used in the study. a) Samples of Lange and Spekk Formation from zone 1-5, b) Sub arkosic sandstone samples from zone 6 and 7, c) Arkosic sandstone samples from zone 8, d) arkosic sandstone samples from zone 9, e) Samples from zone 10, f) Samples from core 6307/07-U-02.

(4a)

Core	Depth (Meters)	Lith.	Detrital grains	Grain size	Sorting	Rounding	Porous or cemented
6307/07-U-02	15.34	Shale	Qtz, fspr, mica	Very fine grained	Poor	Sub rounded sub angular	Aggregate of clay minerals, Porosity (intergranular)
6307/07-U-02	80.97	Shale (Organic rich)	Qtz, fspr	Very fine grained	Poor	Sub rounded sub angular	Clay minerals, Porosity (intergranular)
6307/07-U-02	99.37	Shale (Organic rich)	Qtz, fspr, mica	Very fine grained	Poor	Sub rounded sub angular	Aggregate of clay minerals, porosity (intergranular)

(4b)

Core	Depth (Meters)	Lith.	Detrital grains	Grain size	Sorting	Rounding	Porous or cemented
6307/07-U-02	105.81	Sst	Qtz, mica, fspr, (Microcline)	Medium-coarse grained	Moderate	Sub angular	Dolomite, clay minerals, pyrite porosity(intergranular)
6307/07-U-02	107.77	Sst	Qtz, fspr, mica, glauc, lithic fragments	Medium grained (occasionally coarse)	Moderate-Poor	Sub angular	Carbonate cement porosity(intergranular)
6307/07-U-02	112.25	Sst	Qtz, Fspr, mica, lithic fragments	Fine grained – medium grained	Moderate-poor	Sub rounded-sub angular	Minor carbonate cementation porosity(intergranular)
6307/07-U-02	113.72	Sst	Qtz, fspr, mica, chlorite and glauc	Fine grained, occasionally medium	Moderate	Sub rounded-sub angular	Intergranular Deformation and expansion of feldspar
6307/07-U-02	114.84	Sst	Qtz, fspr, mica, chl, heavy minerals, glauc	Fine grained	Moderate	Sub rounded-sub angular	Porous (intergranular)
6307/07-U-02	116.99	Sst	Qtz, fspr, mica, chlorite, glauc, heavy minerals	Fine grained	Moderate	Rounded-sub rounded	Porous (intergranular)
6307/07-U-02	117.86	Sst	Qtz, fspr, mica, chlorite and glauc	Fine grained	Well-moderate	Rounded-sub rounded	Chlorite, glauc calcite cement. porosity(intergranular)

(4c)

Core	Depth (Meters)	Lith.	Detrital grains	Grain size	Sorting	Rounding	Porous or cemented
6307/07-U-02	119.84	Sst	Qtz, fspr, mica, biotite, chlorite and glauc	Fine grained	Well- moderate	Rounded-sub rounded	Chlorite, glauc, calcite cement, porosity(intergranular)
6307/07-U-02	124.98	Sst	Qtz, fspr, mica, chlorite, biotite and glauc	Fine grained	Moderate-poor	Angular	Chlorite, glauc, calcite cement, porosity(intergranular)
6307/07-U-02	125.60	Sst	Qtz, fspr, mica, chl, biotite and glauc	fine grained	Moderate- poor	Angular	Chlorite, clay minerals, calcite cement, porosity(intergranular)

(4d)

Core	Depth (Meters)	Lith.	Detrital grains	Grain size	Sorting	Rounding	Porous or cemented
6307/07-U-02	129.50	Sst	Qtz, fspr, (microcline), mica	Fine-medium	Well-moderate	Sub rounded-sub angular	Carbonate cement (minor) Porosity (inter + intragranular)
6307/07-U-02	130.35	Sst	Qtz, fspr, mica (few), heavy minerals	Fine grained	Well-moderate	sub rounded	Carbonate cement, Clay minerals, Porosity (inter + intragranular)
6307/07-U-02	135.15	Sst	Qtz, fspr (microcline), mica, chl	Fine grained	Well sorted	Sub rounded	Clay minerals, porosity(intergranular)
6307/07-U-02	136.34	Sst	Qtz, fspr (microcline), glauconite. mica, heavy minerals, plagioclase	Fine-Medium grained	Moderate	Sub-angular	Clay minerals, Carbonate cement, porosity(intergranular)
6307/07-U-02	139.43	Sst	Qtz, fspr, glauc, mica, heavy minerals	Fine – Medium grained	Moderate	Sub-angular	Clay minerals, carbonate cement, porosity (intergranular + intragranular)
6307/07-U-02	141.00	Sst	Qtz, Fspr, heavy minerals	Medium grained	Moderate-Poor	Sub-angular	Minor clay minerals, Carbonate cement porosity(intergranular)
6307/07-U-02	142.55	Sst	Qtz, fspr, chl, minor mica (bending)	Medium grained	Moderate	Sub angular	Clay minerals, carbonate cement, Porosity (inter + intragranular)
6307/07-U-02	148.99	Sst	Qtz, fspr, mica (few)	Fine-Medium	Well-Moderate	Sub rounded-sub angular	Clay minerals, carbonate cement, Porosity (inter + intragranular)
6307/07-U-02	149.81	Sst	Qtz, fspr, mica(few)	Fine grained, occasionally medium	Well-Moderate	Sub rounded-sub angular	Carbonate cement, Porosity (inter + intragranular)
6307/07-U-02	149.51	Sst	Qtz, fspr, mica (few)	Fine grained	Well sorted	Sub rounded	Clay minerals, carbonate cement, Porosity (inter + intragranular)

Core	Depth (Meters)	Lith.	Detrital grains	Grain size	Sorting	Rounding	Porous or cemented
6307/07-U-02	150.79	Sst	Qtz, fspr, mica	Fine grained	Moderate	Sub rounded-sub angular	Clay minerals, carbonate cement, porosity (intergranular + intragranular)
6307/07-U-02	151.58	Sst	Qtz, fspr, mica (few)	Fine grained	Moderate	Sub angular	Clay minerals, carbonate cement, porosity (Intergranular + intragranular)
6307/07-U-02	154.37	Sst	Qtz, minor fspr, mica	Fine grained	Moderate-poor	Sub rounded to sub angular	Clay minerals, carbonate cement, porosity (Intergranular + intragranular), Flspar alteration
6307/07-U-02	156.65	Sst	Qtz, fspr mica	Fine grained	Moderate-Poor	Sub angular	Clay minerals, carbonate cement, porosity (Intergranular + intragranular), Flspar alteration
6307/07-U-02	158.09	Sst	Qtz, fspr	Fine grained, occasionally medium	Moderate	Sub rounded-sub angular	Clay minerals, carbonate cement, porosity (Intergranular + intragranular), Flspar alteration
6307/07-U-02	158.39	Sst	Qtz, fspr, mica	Fine grained	Well-Moderate	Sub rounded Occasionally sub angular	Clay minerals, carbonate cement (minor), porosity (Intergranular + intragranular)
6307/07-U-02	160.86	Sst	Qtz fspr, chl (pore filling)	Fine grained	Moderate-Poor	Sub angular	Carbonate cement, porosity (intergranular)
6307/07-U-02	167.16	Sst	Qtz fspr (some altered), glauc, heavy minerals	Fine-Medium grained	Moderate-Poor	Sub angular	Carbonate cement, porosity (intergranular + intragranular)
6307/07-U-02	170.20	Sst	Qtz, fspr, mica	Very fine-Fine grained	Moderate	Sub rounded-sub angular	Carbonate cemented Porosity (Intergranular)
6307/07-U-02	170.32	Sst	Qtz, fspr, mica (alteration & bending)	Fine grained	Moderate	Sub rounded-sub angular	Carbonate cemented, porosity (intergranular + intragranular)
6307/07-U-02	173.58	Sst	Qtz, fspr, mica,	Fine grained, occasionally	Well-Moderate	Sub rounded	Carbonate cement, clay minerals, porosity

Core	Depth (Meters)	Lith.	Detrital grains	Grain size	Sorting	Rounding	Porous or cemented
				medium grained			(intergranular + intragranular)
6307/07-U-02	176.35	Sst	Qtz, fspr, mica, heavy minerals	Fine-medium grained	Poor	Sub angular -angular	Carbonate cement, clay minerals, porosity (Intergranular + intragranular)
6307/07-U-02	178.39	Sst	Qtz, fspr, chlorite	Fine-medium grained	Poor	Sub rounded	Carbonate cement, clay minerals, porosity (Intergranular + intragranular)

(4e)

Core	Depth (Meters)	Lith.	Detrital grains	Grain size	Sorting	Rounding	Porous or cemented
6307/07-U-02	179.80	Sst	Qtz, fspr, mica, chlorite	Medium grained	Moderate-Poor	Sub rounded-sub angular	Carbonate cement, clay minerals, porosity (Intergranular + intragranular)
6307/07-U-02	180.54	Sst	Qtz, fspr, mica	Fine grained	Well-Moderate	Sub rounded-sub angular	Carbonate cement. less porosity(intergranular)
6307/07-U-02	181.55	Sst	Qtz, fspr, mica, chl	Fine grained	Moderate-Poor	Sub angular to angular	Carbonate cement. less porosity(intergranular)
6307/07-U-02	183.23	Shale	Qtz, fspr	Very fine grained	Moderate-Poor	Sub rounded-sub angular	Carbonate cement. less porosity(intergranular)
6307/07-U-02	183.62	Shale	Qtz, fspr	Very fine grained	Moderate-Poor	Sub angular	Clay minerals

(4f)

Core	Depth (Meters)	Lith.	Detrital grains	Grain size	Sorting	Rounding	Porous or cemented
6307/07-U-3A	12.49	Sst	Qtz, fspr, mica, glauc, lithics	Fine grained	Moderate	Sub rounded-sub angular	Clay minerals, carbonate cement, porosity(intergranular)
6307/07-U-3A	19.29	Sst	Qtz, fspr, mica, lithics	Fine grained	moderate	Sub rounded-sub angular	Clay minerals, carbonate cement, porosity(intergranular)
6307/07-U-3A	19.83	Shale	Qtz, fspr	Very fine grained	Moderate	Sub angular	Clay minerals, carbonate cement
6307/07-U-3A	20.35	Shale	Qtz, fspr	Very fine grained	Moderate-poor	Sub angular	Clay minerals, carbonate cement
6307/07-U-3A	35.34	Shale	Qtz, fspr, mica	Very fine grained	Moderate	Sub rounded	Aggregate of clay minerals
6307/07-U-3A	74.75	Shale	Qtz, fspr	Very fine grained	Poor	surrounded	Aggregate of clay minerals

5.2.2 Modal Analysis results

According to modal analysis, the main detrital grains in the arkosic and subarkosic sandstone samples are quartz, feldspar, mica and trace amount of other minerals (Fig. 20 and 21). The clay minerals are difficult to differentiate by optical point counting because the clay minerals are very fine-grained in nature. The modal porosity value in the studied sample ranges from 10.3 -25.5%. The major factors effecting the porosity in these samples is chlorite cement and pore-filling clay minerals. As during analysis clay was encountered in the samples so the porosity measured by point counting is the minimum porosity value. The dolomite and calcite cement are counted in carbonate cements. The results show that the subarkosic sandstone of the Rogn formation has lowest porosity values due to compaction, pore filling clay and carbonate cement (Fig. 20). The arkosic sandstone shows good porosity values and the porosity is gradually decreasing from the arkosic to the subarkosic sand stone unit. The clay minerals content of sandstones from different depths is shown in Figure 22.

The results of modal analysis are well supported by the XRD results in the respected zone. There are minor differences in quartz, feldspar, and fine minerals values and that are due to inability of separating quartz from feldspar, and distinguishing between fine clay minerals during modal analysis. The results of modal analysis are presented in Table 5.

Table 5 Petrographic composition of sandstone based on modal analysis (300 points, the values are in percentage).

SN	D (m)[1]	Lith[2]	Qtz[3]	Fspr[4]	Mica	Rf[5]	Py[6]	Cc[7]	Chl[8]	Cly[9]	P %[10]	Sum
1	105.81	Sub-arkosic sandstone	64.3	8.5	2.3	0	1.0	11.3	0	3.3	10.3	100
2	116.99	Sub-arkosic sandstone	59.4	8.8	1.3	0	0	4.6	2.3	5.6	18	100
3	125.60	Arkosic sandstone	29.2	33.0	0.3	2.8	0	1.8	0.2	10.5	22.2	100
4	149.51	Arkosic sandstone	35.2	25.8	0.5	2	1.2	4.2	0	7.6	23.5	100
5	156.65	Arkosic sandstone	20.8	30.6	1	0.8	1.9	11	0	8.4	25.5	100
6	173.58	Arkosic sandstone	28.6	28.7	2	1.8	0.5	6.5	0	7.8	24.1	100
7	180.54	Arkosic sandstone	41.1	19.7	3	2.3	0	11	0	4.3	18.6	100
8	181.55	Arkosic sandstone	44.2	20.8	0.5	2	0	5.4	0	3.6	23.5	100
9	183.62	Arkosic sandstone	43.1	26	0.5	1	2.2	2.5	1.2	9.0	14.5	100

[1] Depth
[2] Lithology
[3] Quartz
[4] Feldspar
[5] Rock Fragment
[6] Pyrite
[7] Calcite cement
[8] Chlorite
[9] Clay minerals
[10] Porosity

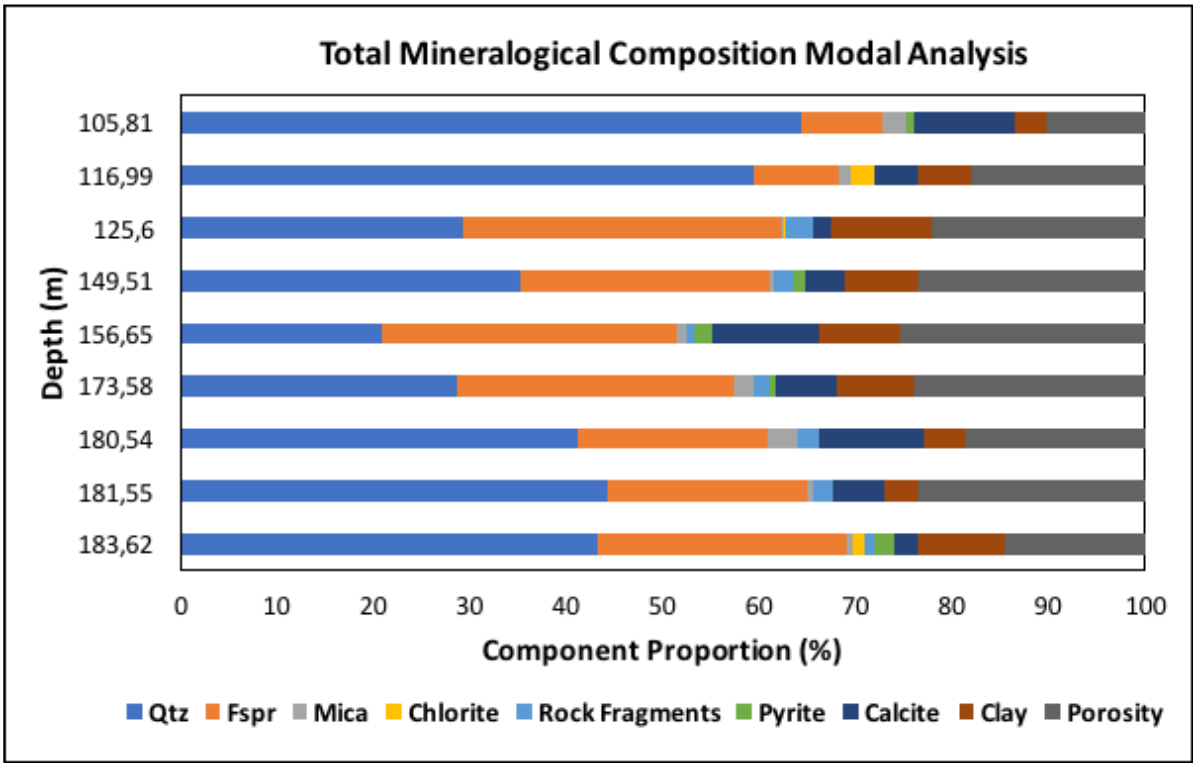

Figure 20 Porosity and Mineralogical composition from Modal analysis. Heavy minerals are counted in rock fragments.

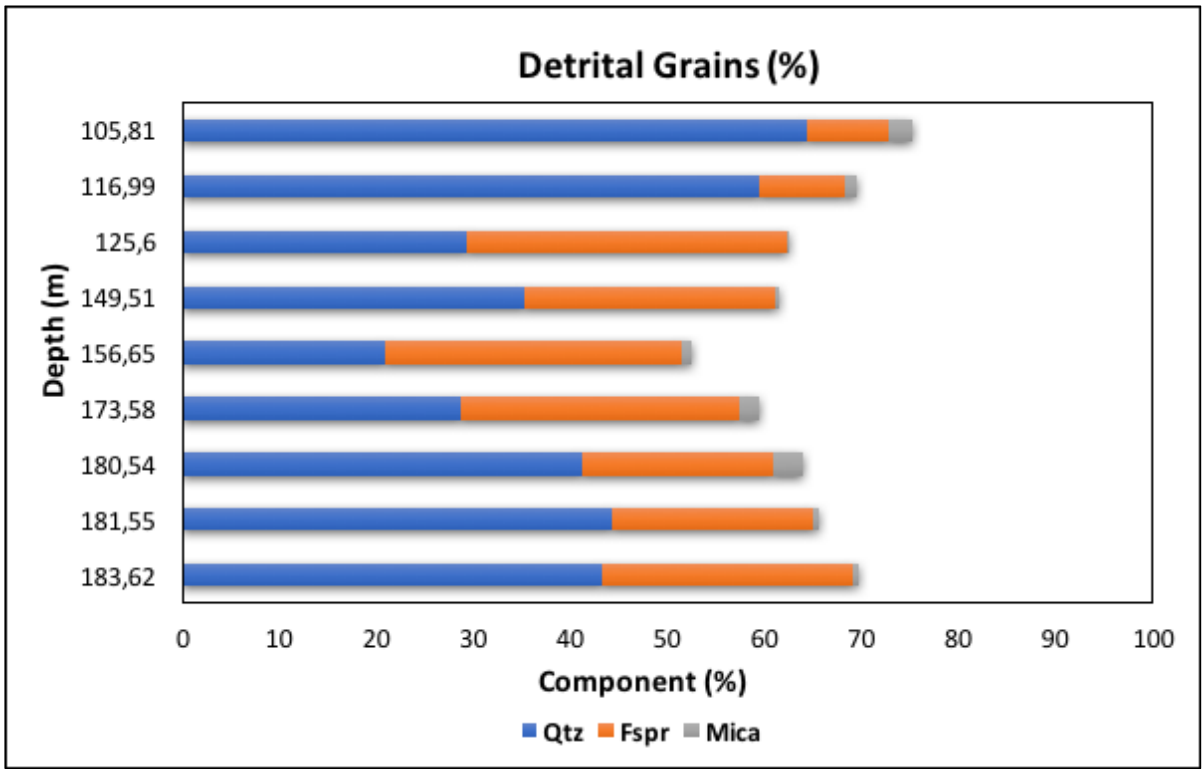

Figure 21 Detrital grains composition from Modal analysis at different depths.

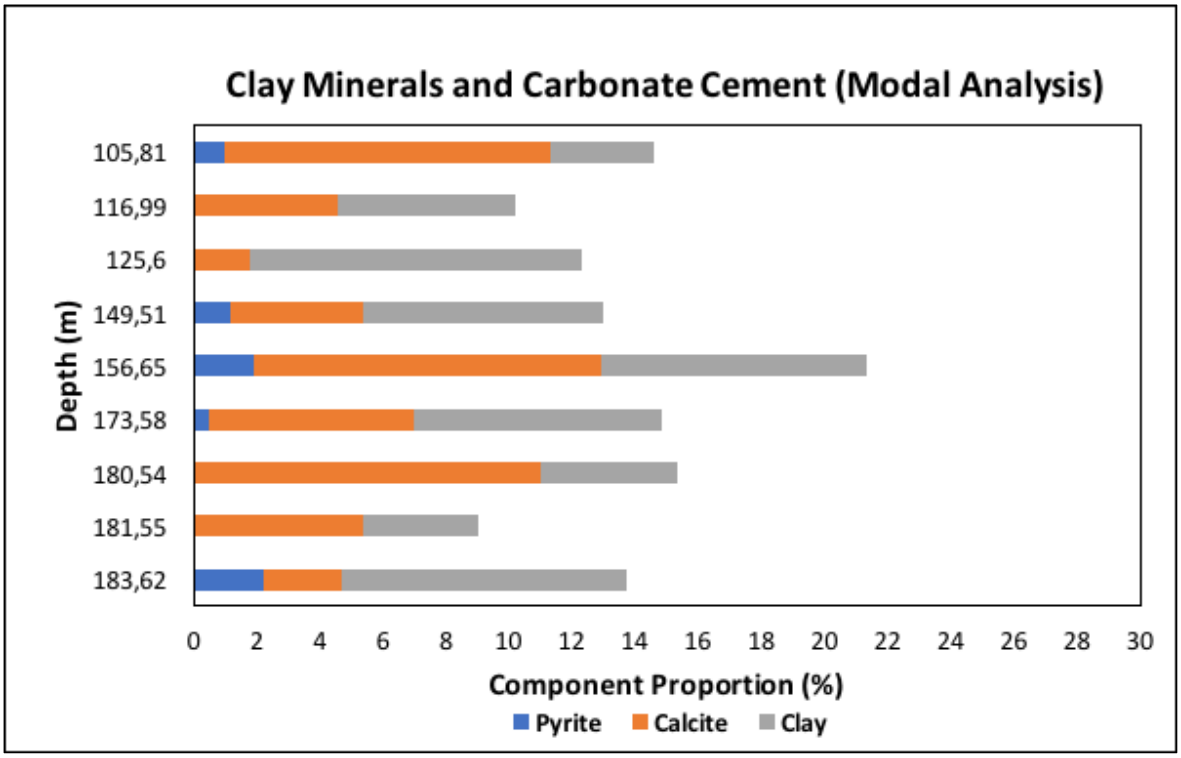

Figure 22 Composition of carbonate cements and clay minerals from Modal analysis at different depths.

5.2.3 X-ray Diffraction Results

XRD of 5 samples from different petrophysical zones is carried out to better understand the lithology and to understand different log responses. Here the major composition of rocks at specific depths is discussed. The results of XRD are given in Table 6 and the total component proportion is shown in Figure 23. The major detrital grains in the samples are quartz, and feldspar with some minor mica, and overall composition of the samples is given in Appendix A.

5.2.3.1 Sample 1 (6307/07-U-03A)

The sample 1 is collected from a depth of 25.05 meters (Zone 4) to investigate the composition of the sandstone. The result from XRD shows that the dominant minerals in the sample are quartz, microcline, kaolinite, muscovite dolomite, pyrite and siderite respectively. As we have no core porosity or permeability data for this depth in the core, we cannot predict the effects of kaolinite, siderite and dolomite on the porosity. But from the thin sections it is evident that these three minerals occur as pore filling cement.

5.2.3.2 Sample 2 (6307/07-U-03A)

The depth of this sample is 61.12 meters (Zone 4, Fig. 16) and represents a siderite nodule. The XRD analysis for this depth was done to check the cause of different response in the petrophysical logs. The analysis shows that the dominant mineral is siderite followed by magnesite, quartz, kaolinite and pyrite.

5.2.3.3 Sample 3(6307/07-U-02)

Sample 3 is taken from a depth of 99.89 (Zone 5, Fig. 12) meters and the results show dominance of quartz, followed by kaolinite, microcline, muscovite and pyrite respectively. Chalcopyrite siderite and jarosite are present in trace amounts.

5.2.3.4 Sample 4(6307/07-U-02)

Sample 4 represents a depth of 105.81meters (Zone 6, Fig. 12). This sample was taken to know the composition of upper subunit of (subarkosic) sandstone which tends to have low microcline content. The results present dominance of quartz, followed by dolomite, microcline, kaolinite and muscovite. Minor calcite, albite and pyrite are also observed in this sample.

5.2.3.5 Sample 5(6307/07-U-02)

Sample 5 represents lower subunit (arkosic) sandstone from a depth of 150.20 meters (Zone 9). The results of the XRD sample shows that sample 5 contains quartz, microcline and kaolinite as dominant minerals. Albite, dolomite, muscovite, calcite and pyrite are present in trace amounts.

The XRD data shows that the kaolinite is the dominant clay mineral. Mixed layer illite/smectite were not detected in the studied sandstone (Rogn Formation).

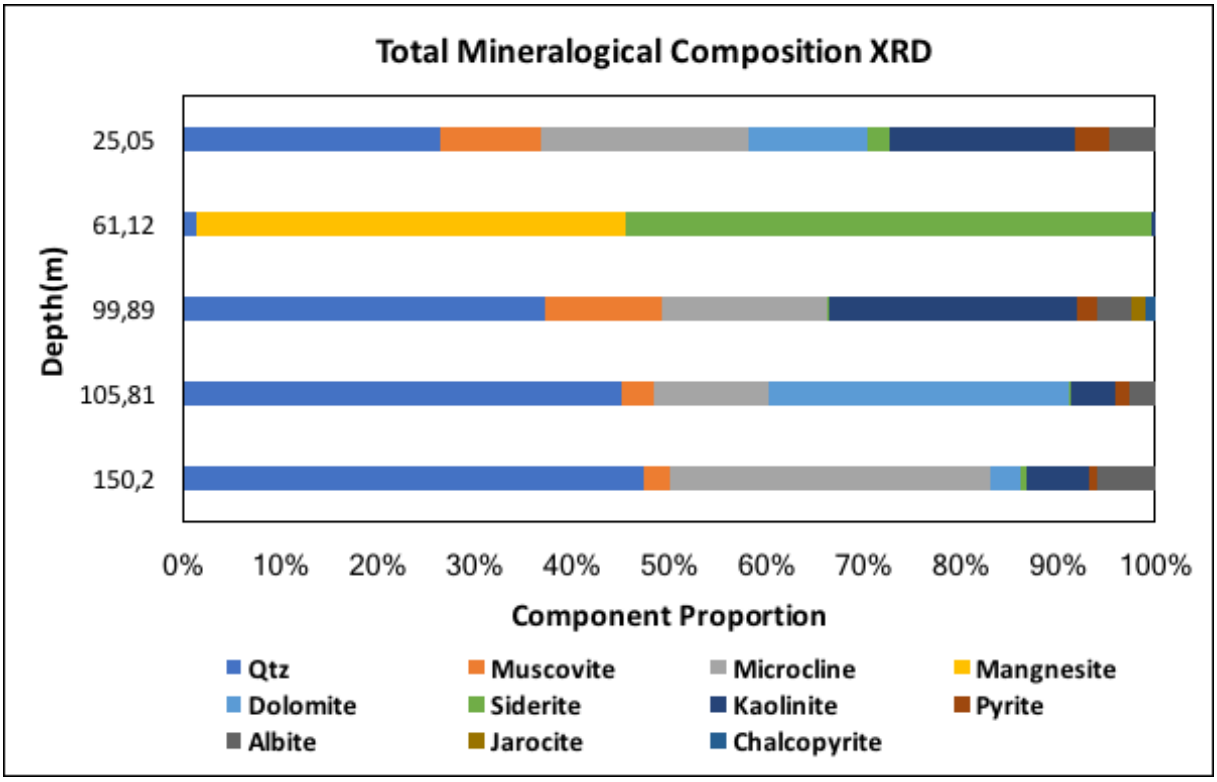

Figure 23 Total Mineralogical composition from XRD analysis.

Table 6 Mineralogical composition from XRD analysis.

D (m)	Qtz	Musc	Microcline	Mng	Dol	Sid[11]	Kao[12]	Pyr[13]	Alb[14]	Jrc[15]	Chlpy[16]
25.05	26.42	10.30	21.40	0	12.24	2.32	19.06	3.42	4.83	0	0
61.12	1.43	0	0	44.15	0	54.01	0.35	0.06	0	0	0
99.89	36.92	11.77	16.88	0	0	0.19	25.17	2.02	3.53	1.42	1.10
105.81	45.11	3.39	11.73	0	31.07	0.19	4.56	1.51	2.62	0	0
150.20	47.14	2.74	32.71	0	3.04	0.63	6.44	0.79	6.03	0	0

[11] Siderite
[12] Kaolinite
[13] Pyrite
[14] Albite
[15] Jarocite
[16] Chalcopyrite

Chapter 6 Discussions

6.1 Diagenetic processes

The sandstone studied in this project is considered as a possible reservoir rock so it is very important to investigate the diagenetic processes that effect reservoir properties. The study shows that authigenic minerals filling the pore spaces is the major phenomenon which effect the reservoir properties. Carbonate cement, clay minerals, minor dolomite and pyrite are some of the authigenic minerals observed in the thin sections. Calcite cement occurs as patchy, and in some thin section slides it also occurs in the form of layers hence resulting in significant reduction of porosity. The most abundant clay mineral is kaolinite and it occurs mostly in the form of pore-filling cement. Very minor chlorite is encountered in a few samples. The formation of kaolinite is a result of alteration of mica and K-feldspar dissolution is observed in the thin sections (Fig.18.).

The authigenic minerals precipitated in the void spaces (pores) of rocks are termed as cement. The most common type of cement in siliclastic rocks are quartz and calcite cement. The texture and composition of the cement depends on pore water chemistry, pressure, temperature and minerology of the rock (Morad, 2009). The thin sections studied in this project show that the Rogn Formation sandstone is calcite cemented. The calcite cement is formed as concretions throughout the sandstone unit. Continuous cemented layer of sandstone is also evident from some samples (e.g. 119.84). Sparitic calcite cement observed can have formed during late diagenesis due to carbonate rich solutions moving through void spaces of the sandstone (Mozley and Davis, 2005). Kaolinite, pyrite, siderite, dolomite, chlorite and glauconite, are also some of the porosity reducing elements. No quartz cement is observed in the thin sections and that is because the calcite cement has filled the intergranular pores during early burial hence restricting quartz cementation. As this sandstone has been buried to a depth of 2 km (Mørk and Johnsen, 2005) it implies that a significant uplift has influenced this unit (Rogn Formation). During uplift the Rogn Formation interacted with meteoric water and some late calcite cement also formed. Observations in the thin sections show calcite cement also as replacive cement i.e., replacing feldspar (Fig. 18). Kaolinite is mostly formed by dissolution and alteration of feldspar (see Chapter 2.3) but some detrital kaolinite is also effecting the porosity of the sandstone unit. The alteration of feldspar is also observed to be impeded by calcite cementation. Volume loss accompanied by porosity reduction as a result of the overburden weight, is termed as compaction.

In sandstones compaction occurs because of rearrangement of grains, pressure solution of minerals, squeezing and bending of ductile elements and brittle fracturing (Boggs, 2009). As the burial depth increases, the overburden weight and temperature increases, hence chemical compaction becomes more effective and results in further loss in porosity. Bending of some ductile grains (mica) in the studied samples and high intergranular volume points towards mechanical compaction (Fig. 18 and Fig. 19). IGV is the summation of pore filling cement and remaining intergranular porosity. This study suggests that calcite cement has filled the intergranular porosity during early diagenetic phase and reduced the mechanical compaction. So, the Rogn Formation in the southern Froan Basin is subjected to minor compaction which is also confirmed by the relatively high porosity values. Considering the initial porosity of sandstones at the time of deposition as 40 % the modal analysis results in the study (Table 5) suggest that subarkosic sandstones underwent more compaction than arkosic sandstones but overall there is minor impact of compaction on porosity loss (Appendix B).

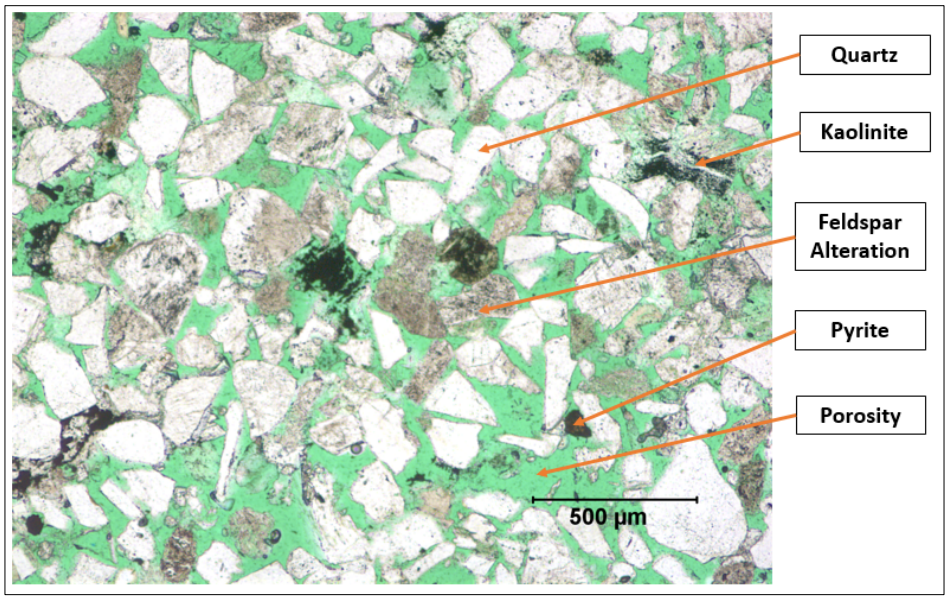

Figure 24 Plain polar, optical micrograph image from 149.81 . Arkosic sandstone (feldspar rich) of Rogn Formation sandstone. Quartz feldspar are the detrital grains dissoloution of feldspar can be observed.

6.2 Detrital grains

The Rogn Formation sandstone contains quartz and feldspar as main detrital grains. Some mica chlorite and glauconite grains are also present. The quartz and feldspar grains are relatively hard so compaction have not significant influence in this study, but mica has shown some bending and fracture. The glauconite is identified based on pellet like shape and green absorption colour and is supposed as indicator of marine depositional environment (Van

Kauwenbergh et al., 1983). The glauconite is observed both as pore filling cement and reworked detrital grains.

6.3 Textural maturity

The textural maturity of studied sandstone is interpreted based on Folk (1951). Three parameters are considered in defining textural maturity: a) clay removal), b) good sorting in the part where there is no clay, c) Rounding (reflecting maximum energy required). Based on these the textural maturity of sandstones is divided into 4 stages and is shown in Figure 25. (Folk, 1951).

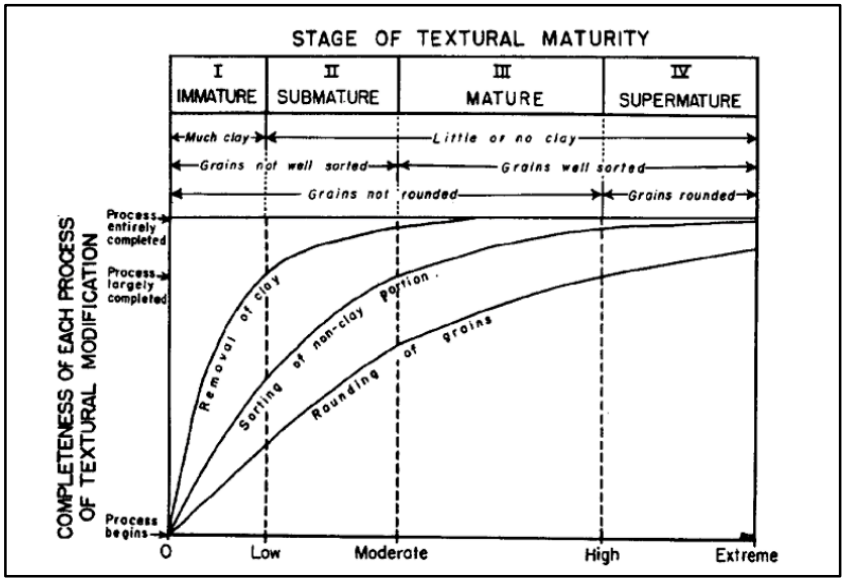

Figure 25 Classification of textural maturity (Folk, 1951).

1) Immature stage: Sediments contain clay and mica, and the portion without clay is poorly sorted with angular grains.
2) Sub-mature stage: Very little or no clay, non-clay part is poorly sorted and the grains are angular. Towards the end of this stage sediments become well sorted.
3) Mature stage: No clay, well sorted and angular grains in this stage.
4) Super mature stage: No clay, well sorted, and well-rounded grains represent the super mature stage.

Based on the clay content, grain size and sorting the studied samples suggest that the Rogn Formation encountered in the Froan Basin is texturally and compositionally sub-mature to immature. Immature sandstone samples show poorly sorted, angular sand grains and clay matrix is also present. Immature sandstones are the characteristic of the environments in which sediment is deposited and later is not effected by currents or waves i.e. lagoons, below wave base etc. But these can also be deposited in the subaerial environment and the areas where sediment input is exceeding weathering rate (Boggs, 2006). Sub mature sandstones are

deposited because of clay matrix removal due to current action. These sandstones are moderate-poorly sorted and are commonly formed as shallow sub marine sands aided by unidirectional currents.

6.4 Classification of sandstones

The sandstone is classified based on Dott's (1964) classification scheme using the modal analysis data. This classification is based on the sand framework grain content and lithic components. Heavy minerals and rock fragments are included in lithic fragments, whereas sand framework grains contain quartz and feldspar. The studied arkosic sandstones in zone 8 and 9 are feldspar rich, coarse-grained sandstones. The dominant mineral is quartz, but in some cases the feldspar content is exceeding the quartz content. In general, a sandstone is classified as arkose if it is containing at least 25% feldspar and the feldspar content is exceeding the lithic fragments. Similarly, in subarkosic arenite (subarkose), the feldspar content is ranging from 5-15% and is exceeding the lithic rock fragments (Folk, 1951). Based on the petrographical analysis the sandstone units investigated in this project are divided into two subunits arkosic and subarkosic sandstones (Fig 26). The thickness of these units is measured with the aid from thin sections and petrophysical data.

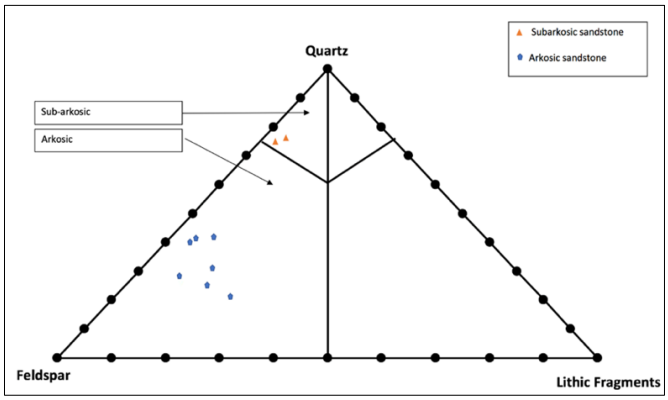

Figure 26 Qtz- fspr-lithcs plot of the Rogn Formation sandstone samples (Dott Jr, 1964).

6.5 Porosity and Permeability

Primary porosity is a type of porosity affiliated with the original depositional texture of the sediments i.e. the pore space inbetween the matrix and within the detrital grains. This type of porosity is termed as primary intergranular porosity. The porosity formed due to dissolution of feldspar and calcite cement is termed intragranular porosity. The porosity in the Rogn Formation sandstone is mainly intergranular and some secondary intragranular porosity (dissolution porosity) in feldspar. The secondary pores are partly filled by authigenic clays and calcite cement resulting in porosity reduction. Among the clay minerals authigenic kaolinite is

the most abundant porosity and permeability reducing element. The range of the analyzed modal porosity of the Rogn Formation sandstone is 10.3-25.5%. The permeability in sandstones is sharply decreasing in zone 7 and zone 8 and this can be due to plagioclase dissolution, as it was associated with the formation of kaolinite (Fig. 27), hence resulting in reduction of permeability. The porosity in these zones is 18-22 % that suggests that the kaolinite clay has blocked the pore spaces, so although there is good porosity the permeability values are low.

6.6 Porosity preserving mechanism in the Rogn Formation

The porosity/depth relationships are based on parameters related to the burial history i.e., pressure and temperature. The texture and minerology also have a significant impact on this relationship. From the literature the porosity reduction in sediments buried down to a depth of 2.5 to 3.0 km is mainly due to mechanical compaction (Ramm and Bjørlykke, 1994). As this area is buried to a depth of 2 km (Mørk and Johnsen, 2005), so mechanical compaction has effected the porosity, but the sandstone samples show high inter granular volume which means that the porosity loss by mechanical compaction was seized by the early calcite cementation (Fig 27). Secondary dissolution pores are formed during late diagenesis due to dissolution of detrital feldspar and calcite cement which resulted in enhancement of porosity. The acidic pore-fluids rich in organic and inorganic acids, as well as the meteoric waters, are the main dynamic force and fluid medium for the dissolution of fragments in the sandstones.

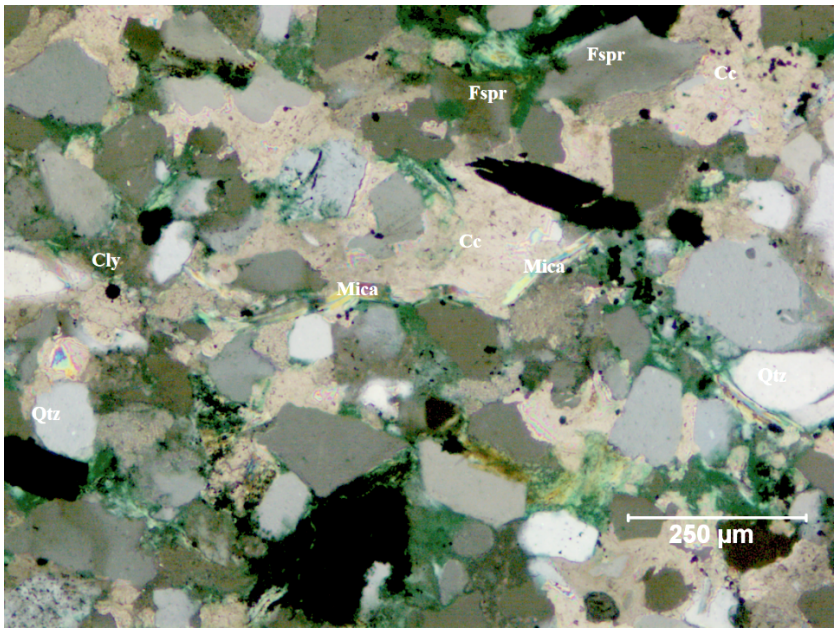

Figure 27 Cross Polar, Optical micrograph image from 105.81 m. Sub-arkosic sandstone of the Rogn Formation. Cc : Carbonate cement (calcite), Qtz: quartz, Fspr: Feldspar, Mica (Muscovite). Mica shows minor bending due to compaction.

6.7 Provenance and depositional environment

Feldspars are one of the most common minerals in metamorphic and igneous rocks. As feldspars are less stable than quartz on near surface conditions they only make 10 to 15% of all sandstones (Burley and Worden, 2009). Arkosic sandstones show provenance from weathering of feldspar-rich metamorphic and/or igneous rocks mainly granitic rocks (Folk, 1980). The well-preserved feldspar rich composition suggests relatively rapid deposition. The feldspar minerology of the arkosic sandstones (mostly microcline) combined with heavy minerals (zircon, tourmaline) suggests granitic source rocks. The subarkosic sandstones in the study are also representing a provenance from dominantly granitic rocks, whereas the rock fragments in the sandstone are pointing to provenance from metamorphic rocks as well. These results are in line with the interpretation of Mørk & Johnsen (2005).

The depositional environment of the Rogn Formation sandstone is interpreted as shallow marine bar deposits (Dalland et al., 1988). The presence of glauconite in the Rogn Formation deposited in the Froan basin supports a marine environment. As the sandstone is deposited within the organic rich shales of Spekk Formation (Dalland et al., 1988), so this represents a change of depositional environment. This change of environment can be due to change of sea level. A possible explanation is that the sandstones are deposited during sea level fall when erosion was exceeding the sedimentation rate. Brekke et al. (2001) report changes of sea level during the late Jurassic which is supporting this interpretation. The shales of Spekk Formation are organic rich representing outer shelf environments of deposition (Fig. 28).

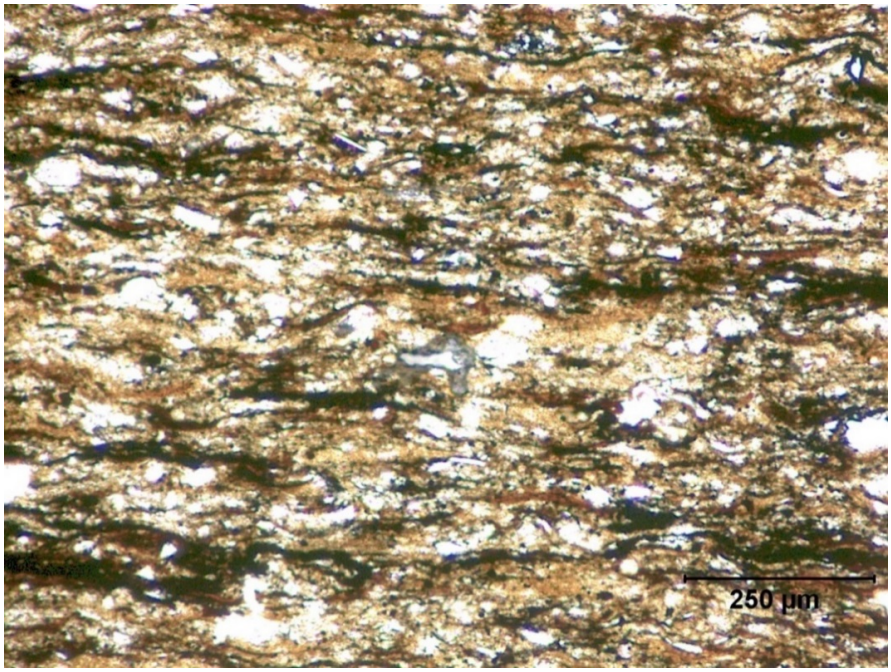

Figure 28 Optical micro graph image of organic rich shale (Spekk Formation) from 80.97 m.

6.8 Relationship between petrophysical and petrographical analysis

The petrophysical analysis and petrographical analysis of well 6307/07-U-02 are supporting each other in lithology interpretation. In the petrophysical results Zone 1 to Zone 5 are interpreted as shale which is in line with the petrography results, but from zones 6-9 sandstone is interpreted with high gamma ray values. The petrography of sandstone samples from these zones shows high feldspar and clay content. Clay minerals and high feldspar contents result in increase of gamma ray values. Kaolinite and smectite clays are rich in thorium and illite contains potassium, these elements are radioactive hence influence the gamma ray reading (Diaz et al., 2013). Thus, petrography confirms the presence of both these elements responsible for high gamma ray values. The petrophysical analysis shows slightly higher values of porosity than the petrography results (modal analysis), because of considerable amount of clay minerals. Due to lack of petrophysical data and core porosity/permeability data in well 6307/07-U-03A, only lithology of the zones 1-4 is interpreted there and correlated with the petrography results. No porosity permeability calculations are carried out for this well.

Slight increase in sonic log velocity was noted in some intervals and were considered as some diagenetic effects. The thin sections from those intervals shows calcite cementation so it is concluded that the decrease in sonic log response in the sandstone unit is due to calcite cementation.

There is minor difference in porosity calculations from the two methods, where petrophysical analysis shows sandstone porosities ranging from 16-30% and petrographical analysis display 10.3-25.5% porosities. This difference in porosity values can be because of inability to calculate porosity associated with clay minerals during modal analysis.

Chapter 7 Conclusions

The focus of the study was to investigate reservoir quality of the Upper Jurassic Rogn Formation sandstones based on shallow cores in the Froan Basin. The Rogn Formation is deposited within the organic rich shales of the Spekk Formation in the area. The sandstones are compositionally and texturally sub mature to immature. Based on mineralogical variation the Rogn formation sandstones are divided into arkosic and subarkosic. The major detrital grains are quartz, feldspar and mica. Chlorite and some heavy minerals are also present as detrital grains. The difference between the two subunits is that sub-arkosic sandstones shows high mica and low microcline content whereas the arkosic sandstones represents high microcline and low mica content. The subarkosic sandstones are medium to coarse grained and moderate to poorly sorted whereas, the arkosic sandstones are fine to medium grained and well to moderately sorted.

The porosity is mainly intergranular. Some intragranular porosity is due to dissolution of feldspar, and the secondary pores are then partially filled by clay minerals and calcite cement. The porosity values from modal analyses ranges from 10.3 to 25.5% and the major porosity reducing factors in the studied wells are compaction, calcite cementation and authigenic clay minerals. Compaction has very small impact on porosity reduction as only minor bending and deformation has been noticed in the sandstones. Small quantities of dolomite, siderite, chlorite and pyrite are also present as pore filling cements. Kaolinite is the major porosity and permeability reducing clay mineral but XRD results depict the presence of chlorite and illite also as clay minerals. Kaolinite is formed due to dissolution and alteration of feldspar but detrital kaolinite filling the pores is also observed. Early calcite cementation stopped the quartz cementation and due to this calcite cementation compaction was also reduced, so this cementation also helped in preserving porosity.

In petrophysical analysis 10 zones were interpreted, from zone 1-5 the lithology is shale. From zone 6-9 sandstone is encountered. The lithology interpretation is confirmed by the petrographical analysis. The porosity values range from 18-30% and the permeability values of this sandstone are ranging from 5-330 milli Darcy. The Zone 9 in the studied well has porosity 30% and permeability values are averaging 330 mDarcy hence depicting good reservoir properties but no hydrocarbon zone is present. The subarkosic sandstone has low porosity and permeability as compared to arkosic sandstone due to compaction.

References

Aanstad, K., Gabrielsen, R., Hagevang, T., Ramberg, I., and Torvanger, O., Correlation of offshore and onshore structural features between 62 N and 68 N, Norway, in Proceedings, Norwegian Symposium on Exploration, Bergen1981, p. 1-25.

Barbara, 2017, X-ray Powder Diffraction (XRD), Volume 2017: Barbara L Dutrow, Louisiana State University , Christine M. Clark, Eastern Michigan University.

Bjorlykke, K., 1979, Cementation of sandstones: discussion: Journal of Sedimentary Research, v. 49, no. 4.

Blystad, P., Brekke, H., and Faerseth, R. B., 1995, Structural Elements of the Norwegian Continental Shelf. Pt. 2. The Norwegian Sea Region, Norwegian Petroleum Directorate.

Bøe, R., Fossen, H., and Smelror, M., 2010, Mesozoic sediments and structures onshore Norway and in the coastal zone: Norges geologiske undersøkelse Bulletin, v. 450, p. 15-32.

Boggs, S., 2006, Principles of sedimentology and stratigraphy, Pearson Prentice Hall.Cambridge University Press.

Brekke, H., 2000, The tectonic evolution of the Norwegian Sea continental margin, with emphasis on the Voring and More basins: Special Publication-Geological Society of London, v. 167, p. 327-378.

Brekke, H., Dahlgren, S., Nyland, B., and Magnus, C., The prospectivity of the Vøring and Møre basins on the Norwegian Sea continental margin, in Proceedings Geological Society, London, Petroleum Geology Conference series1999, Volume 5, Geological Society of London, p. 261-274.

Brekke, H., and Riis, F., 1987, Tectonics and basin evolution of the Norwegian shelf between 62 N and 72 N: Norsk Geologisk Tidsskrift, v. 67, p. 295-322.

Brekke, H., Sjulstad, H. I., Magnus, C., and Williams, R. W., 2001, Sedimentary environments offshore Norway—an overview: Norwegian Petroleum Society Special Publications, v. 10, p. 7-37.

Bukovics, C., Cartier, E., Shaw, N., and Ziegler, P., 1984, Structure and development of the mid-Norway continental margin, Petroleum geology of the North European margin, Springer, p. 407-423.

Burley, S., and Worden, R., 2009, Sandstone Diagenesis: Recent and Ancient (Reprint Series 4 of the IAS), John Wiley & Sons.

Dalland, A., Worsley, D., and Ofstad, K., 1988, A Lithostratigraphic Scheme for the Mesozoic and Cenozoic and Succession Offshore Mid-and Northern Norway, Oljedirektoratet.

Deegan, C. t., and Scull, B. J., 1977, A standard lithostratigraphic nomenclature for the Central and Northern North Sea, HMSO.

Diaz, H. G., Lewis, R., and Miller, C., Evaluating the impact of mineralogy on reservoir quality and completion quality of organic shale plays, in Proceedings AAPG Rocky Mountain Section Meeting, Salt Lake City, Utah2013.

Dott Jr, R. H., 1964, Wacke, Graywacke and Matrix--What Approach to Immature Sandstone Classification?: Journal of Sedimentary Research, v. 34, no. 3.

Fagerland, N., 1990, Mid-Norway shelf-hydrocarbon habitat in relation to tectonic elements: Norsk Geologisk Tidsskrift, v. 70, p. 65-79.

Faleide, J. I., Tsikalas, F., Breivik, A. J., Mjelde, R., Ritzmann, O., Engen, O., Wilson, J., and Eldholm, O., 2008, Structure and evolution of the continental margin off Norway and the Barents Sea: Episodes, v. 31, no. 1, p. 82-91.

Folk, R. L., 1951, Stages of textural maturity in sedimentary rocks: Journal of Sedimentary Research, v. 21, no. 3.

Gabrielsen, R., Odinsen, T., and Grunnaleite, I., 1999, Structuring of the Northern Viking Graben and the Møre Basin; the influence of basement structural grain, and the particular role of the Møre-Trøndelag Fault Complex: Marine and Petroleum Geology, v. 16, no. 5, p. 443-465.

Gjelberg, J., Enoksen, T., Kj, P., Mangerud, G., Martinsen, O., Roe, E., and Vágnes, E., 2001, The Maastrichtian and Danian depositional setting, along the eastern margin of the Møre Basin (mid-Norwegian Shelf): implications for reservoir development of the Ormen Lange Field: Norwegian Petroleum Society Special Publications, v. 10, p. 421-440.

Grogan, P., Østvedt-Ghazi, A.-M., Larssen, G., Fotland, B., Nyberg, K., Dahlgren, S., and Eidvin, T., Structural elements and petroleum geology of the Norwegian sector of the northern Barents Sea, in Proceedings Geological Society, London, Petroleum Geology Conference series1999, Volume 5, Geological Society of London, p. 247-259.

Halland, E., Gjeldvik, I., Johansen, W., Magnus, C., Meling, I., Pedersen, S., Riis, F., Solbakk, T., and Tappel, I., 2011, CO2 Storage Atlas Norwegian North Sea: Norwegian Petroleum Directorate, PO Box, v. 600.

Halland, E., Mujezinovic, J., Riis, F., BJØRNESTAD, A., MELING, I., GJELDVIK, I., TAPPEL, I., BJØRHEIM, M., RØD, R., and PHAM, V., 2014, CO 2 Storage Atlas: Norwegian Continental Shelf: Norwegian Petroleum Directorate, Stavanger, Norway.

Hill, R., Tsambourakis, G., and Madsen, I., 1993, Improved petrological modal analyses from X-ray powder diffraction data by use of the Rietveld method I. Selected igneous, volcanic, and metamorphic rocks: Journal of Petrology, v. 34, no. 5, p. 867-900.

Hollander, N., 1982, Evaluation of the hydrocarbon potential offshore mid Norway: Oil & Gas Journal, v. 80, no. 15, p. 168-&.

Isaksen, D., and Tonstad, K., 1989, A revised Cretaceous and Tertiary lithostratigraphic nomenclature for the Norwegian North Sea, Norwegian Petroleum Directorate.

Langrock, U., and Stein, R., 2004, Origin of marine petroleum source rocks from the Late Jurassic to Early Cretaceous Norwegian Greenland Seaway—evidence for stagnation and upwelling: Marine and Petroleum Geology, v. 21, no. 2, p. 157-176.

Lundin, E., Polak, S., Bøe, R., Zweigel, P., Lindeberg, E., and Smelror, M., 2005, Storage potential for CO2 in the Froan Basin area of the Trøndelag Platform, Mid-Norway: NGU Report.

McBride, E. F., 1989, Quartz cement in sandstones: a review: Earth-Science Reviews, v. 26, no. 1-3, p. 69-112.

Morad, S., 2009, Carbonate Cementation in Sandstones: Distribution Patterns and Geochemical Evolution (Special Publication 26 of the IAS), John Wiley & Sons.

Morad, S., Al-Ramadan, K., Ketzer, J. M., and De Ros, L., 2010, The impact of diagenesis on the heterogeneity of sandstone reservoirs: A review of the role of depositional facies and sequence stratigraphy: AAPG bulletin, v. 94, no. 8, p. 1267-1309.

Mørk, M. B. E., and Johnsen, S., 2005, Jurassic sandstone provenance and basement erosion in the Møre margin–Froan Basin area: Norges geologiske undersøkelse Bulletin, v. 443, p. 5-18.

Mørk, M. B. E., Vigran, J. O., Smelror, M., Fjerdingstad, V., and Bøe, R., 2003, Mesozoic mudstone compositions and the role of kaolinite weathering-a view from shallow cores in the Norwegian Sea (Møre to Troms): Norwegian Journal of Geology/Norsk Geologisk Forening, v. 83, no. 1.

Mozley, P. S., and Davis, J. M., 2005, Internal structure and mode of growth of elongate calcite concretions: Evidence for small-scale, microbially induced, chemical heterogeneity in groundwater: Geological Society of America Bulletin, v. 117, no. 11-12, p. 1400-1412.

Müller, R., Ngstuen, J. P., Eide, F., and Lie, H., 2005, Late Permian to Triassic basin infill history and palaeogeography of the Mid-Norwegian shelf—East Greenland region: Norwegian Petroleum Society Special Publications, v. 12, p. 165-189.

NPD, 2016, Petroleum resources on the Norwegian continental shelf 2016, Volume 2017, NPD.

Pechnig, R., Haverkamp, S., Wohlenberg, J., Zimmermann, G., and Burkhardt, H., 1997, Integrated log interpretation in the German Continental Deep Drilling Program: lithology, porosity, and fracture zones: Journal of Geophysical Research: Solid Earth, v. 102, no. B8, p. 18363-18390.

Ramm, M., and Bjørlykke, K., 1994, Porosity/depth trends in reservoir sandstones: Assessing the quantitative effects of varying pore-pressure, temperature history and mineralogy, Norwegian Shelf data: Clay minerals, v. 29, no. 4, p. 475-490.

Rhys, G., and Sciences, I. G., 1974, Proposed standard lithostratigraphic nomenclature for the southern north sea and an outline structural nomenclature of the whole of the (UK) North Sea: Inst.Geol. sci., Report No 74/08,.

Saxena, P., 2016, Play based evaluation of the eastern margin of Nordland Ridge, Norwegian Sea: University of Stavanger, Norway.

Schneider, F., Potdevin, J., Wolf, S., and Faille, I., 1996, Mechanical and chemical compaction model for sedimentary basin simulators: Tectonophysics, v. 263, no. 1-4, p. 307-317.

Smelror, M., Jacobsen, T., Rise, L., Skarbø, O., Verdenius, J., and Vigran, J., 1994, Jurassic to Cretaceous stratigraphy of shallow cores on the Møre Basin Margin, Mid-Norway: Norsk Geologisk Tidsskrift, v. 74, p. 89-107.

Spencer, A. M., 1984, The Petroleum Geology of the North European Margin, Springer.

Van Kauwenbergh, S. J., Cathcart, J. B., and McClellan, G. H., 1983, Mineralogy and alteration of the phosphate deposits of Florida: a detailed study of the mineralogy and chemistry of the phosphate deposits of Florida, US Government Printing Office, v. 1914-1917.

Vollset, J., and Doré, A. G., 1984, A revised Triassic and Jurassic lithostratigraphic nomenclature for the Norwegian North Sea, Oljedirektoratet.

Wilson, M. J., Rock-forming Minerals: Clay Minerals. Sheet Silicates. Volume 3C2013, Geological Society of London.

Worden, R., and Burley, S., 2003, Sandstone diagenesis: the evolution of sand to stone: Sandstone Diagenesis: Recent and Ancient, v. 4, p. 3-44.

Zabanbark, A., 2013, Oil and gas bearing in Norwegian Sea basins: Oceanology, v. 53, no. 4, p. 491-497.

Appendix A

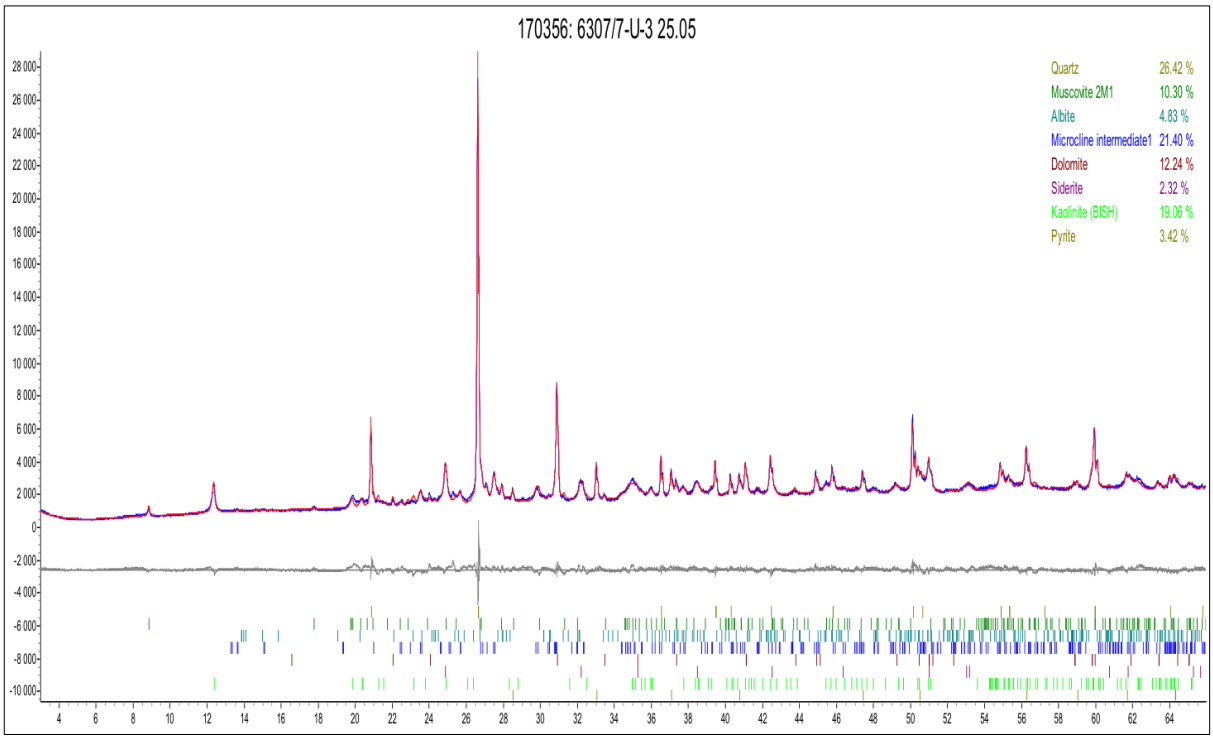

Figure A. 1 XRD result of Sample 1

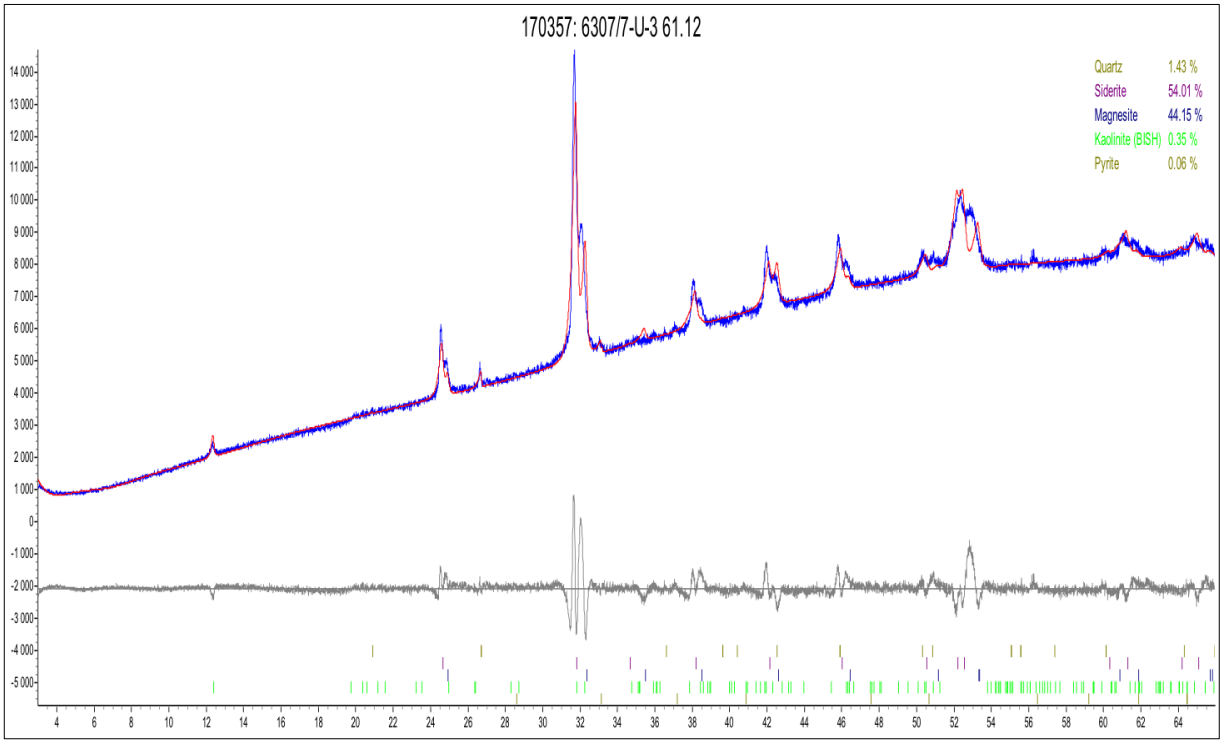

Figure A. 2 XRD result of Sample 2.

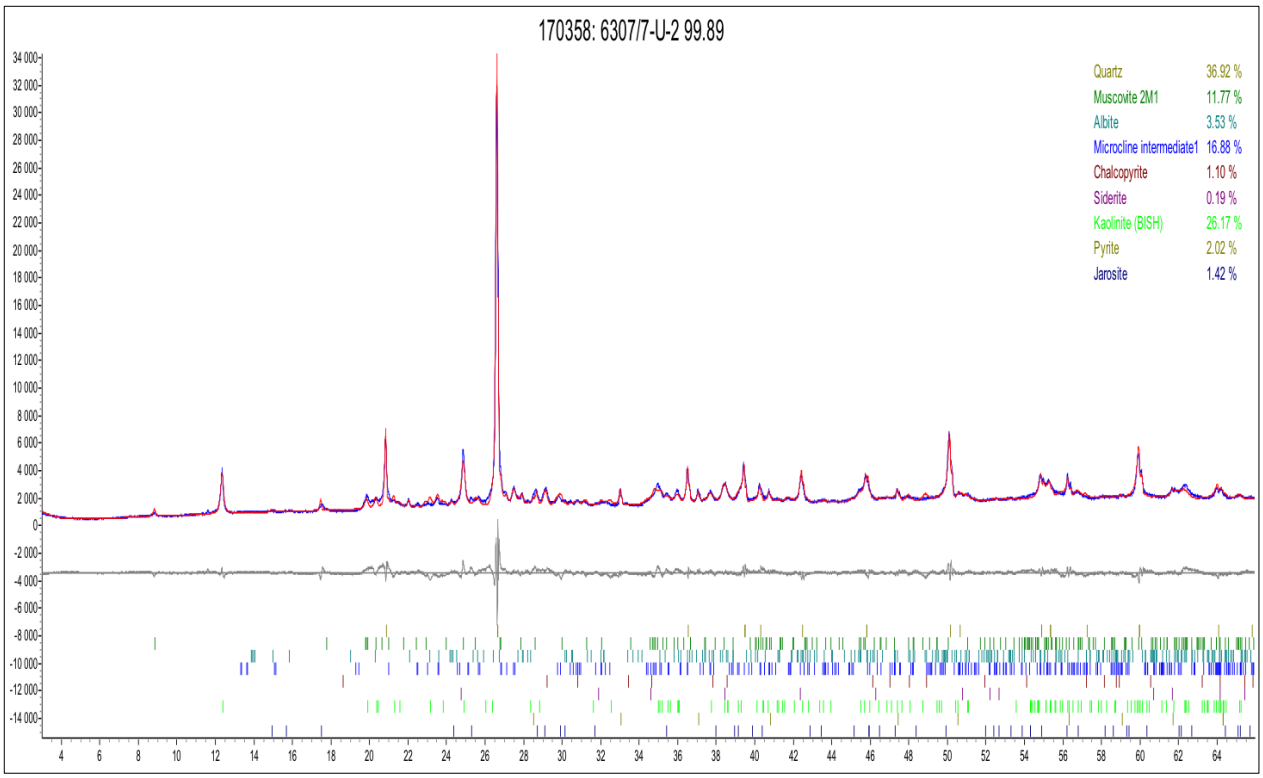

Figure A. 3 XRD result of Sample 3.

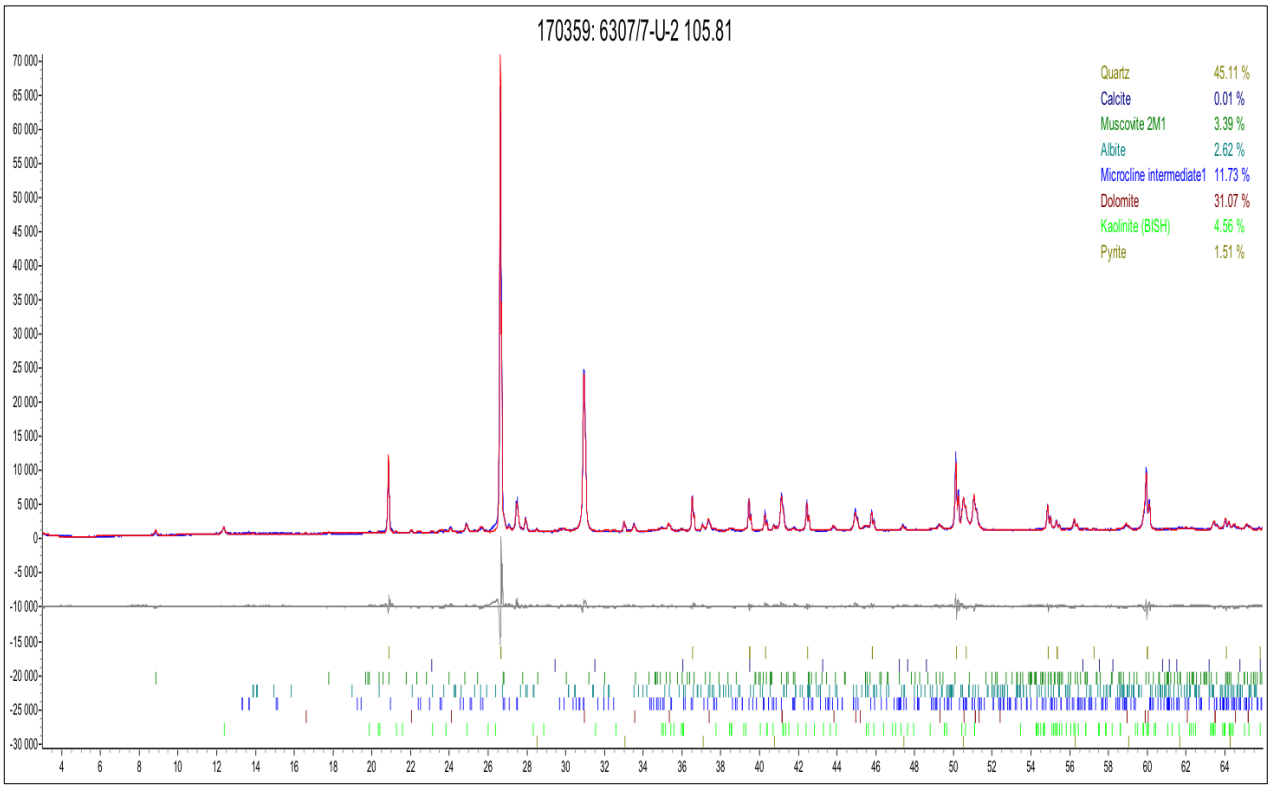

Figure A. 4 XRD result of sample 4

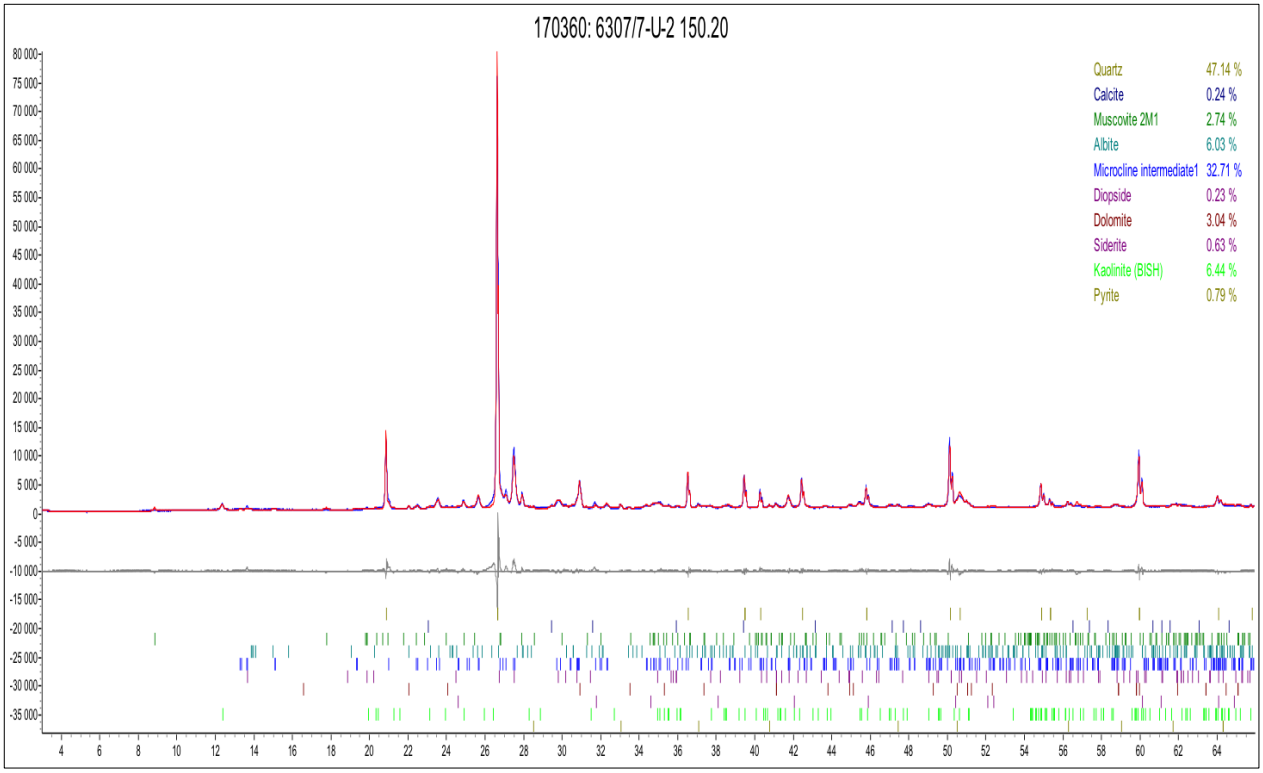

Figure A. 5 XRD result of Sample 5.

Appendix B

Table B. 1 shows inter granular volume of the samples from different depths.

Depth (m)	Intergranular porosity	Carbonate cement	Clay minerals	Pyrite	Chlorite	IGV (Intergranular volume)
105,81	10,3	11,3	3,3	1	0	25,9
116,99	18	4,6	5,6	0	2,3	30,5
125,6	22,2	1,8	10,5	0	0,2	34,7
149,51	23,5	4,2	7,6	1,2	0	36,5
156,65	25,5	11	8,4	1,9	0	46,8
173,58	24,1	6,5	7,8	0,5	0	38,9
180,54	18,6	11	4,3	0	0	33,9
181,55	23,5	5,4	3,6	0	0	32,5